

## Absorption Spectra of Cr<sup>3+</sup> in Al<sub>2</sub>O<sub>3</sub>

### Part A. Theoretical Studies of the Absorption Bands and Lines

By Satoru SUGANO

*Department of Physics, Faculty of Science,  
University of Tokyo, Tokyo*

and Yukito TANABE

*Department of Applied Physics, Faculty of Engineering,  
University of Tokyo, Tokyo*

(Received, April 5, 1958)

In the frame-work of the crystalline field theory, the excited states of Cr<sup>3+</sup> in Al<sub>2</sub>O<sub>3</sub> and the optical transitions to these states are studied taking into account the effect of trigonal field and spin-orbit interaction. Initial splittings and optical anisotropies of the broad band (transitions to quartet states) and the sharp lines (transitions to doublet states) are examined. For the sharp lines, the Zeeman effect is also examined and the Zeeman patterns are predicted. Comparing these theoretical results with those of the experimental ones given in Part B, the assignments of U, Y bands and R<sub>1</sub>, R<sub>2</sub>, B<sub>1</sub>, B<sub>2</sub> lines have been established. It is shown that the g-shifts of the excited doublets observed in the Zeeman patterns can also be explained under such assignments. It is also shown that the experimental data of the optical absorption can be reasonably connected to those of the paramagnetic resonance absorption.

#### § 1. Introduction

In the last several years, it has been believed by many authors that the optical spectra of normal complex ions of the first transition-metal elements are reasonably explained by the crystal-field or the ligand-field theory of d-electrons<sup>1)</sup>. It is true that the theory predicted the positions of the absorption bands and lines in agreement with the experiments and gave reasonable order of magnitudes for the intensities and widths. However, we still feel that a more definite evidence than those mentioned above is needed to confirm the theory because the number of the observed absorption bands in the individual complex is rather limited and the detailed analyses of the sharp absorption lines have not yet been made. The main purpose of this series of papers is to give a more sound foundation to the crystal field theory of optical absorption than that previously established by examining, both theoretically and experimentally, the details of the optical spectra of ruby.

The reason why we adopt ruby for this purpose is as follows:

Similarity of the spectra to those of Cr alum: A single crystal of ruby whose colour is, as well known, due to Cr<sup>3+</sup> impurities in

Al<sub>2</sub>O<sub>3</sub> crystal shows similar spectra to those of Cr alum; The spectra in the visible region consist of two bands (obs. max. at  $\sim 18000 \text{ cm}^{-1}$  and  $\sim 25000 \text{ cm}^{-1}$ ) and of several groups of lines situated at  $\sim 14400 \text{ cm}^{-1}$  and  $\sim 21000 \text{ cm}^{-1}$ . From the knowledge of the crystal structure (§ 2), we can see that Cr<sup>3+</sup> impurities which substitute Al<sup>3+</sup> ion of Al<sub>2</sub>O<sub>3</sub> are surrounded almost octahedrally by six nearest O<sup>2-</sup> ions and are therefore subject to a strong cubic field just as in the case of Cr<sup>3+</sup> ion in Cr alum. In addition to this cubic field, there is a relatively strong trigonal field whose axis is the optic axis C<sub>3</sub>. Thus we can safely assume that the same treatment will be applicable to both Cr alum and ruby to explain their optical spectra.

Contrast to Cr alum: It has a distinct optic axis and, as will be reported in a later paper, shows a remarkable optical anisotropy which is not observed in the case of Cr alum. It is stable both at high and low temperatures so that we can get much informations on the optical behaviours at these temperatures, while Cr alum is unstable at high temperature and shows phase-transition at low temperature which complicates the interpretation of the line spectra of Cr alum greatly. It shows a

relatively strong luminescence in the red region where the sharp line absorptions are observed. This luminescence is absent in Cr alum.

Thus ruby can provide us with more useful and definite informations than Cr alum that has been regarded as a representative material with its abundance of spectra, the elucidation of which has been the success of the crystal field theory.

Of course, ruby, as a diluted antiferromagnetic substance  $\text{Cr}_2\text{O}_3$ , has many interesting problems in its own and thus the present study may also be interesting from another point of view.

Experimentally, we have a fairly abundant knowledge about ruby. Deutchbein<sup>2)</sup> has examined many narrow spectra of both absorption and emission many years ago and Lehmann<sup>3)</sup> has performed an elaborate experiment on the Zeeman effect of the characteristic doublet  $R_1$  and  $R_2$  observed at  $\sim 14400 \text{ cm}^{-1}$ . There remain, however, some doubts with respect to the quantitative aspect of his experiment. In view of the importance of the Zeeman effect in the analysis of the line spectra, measurements of the Zeeman effect were made again under experimentally better conditions both for the line spectra of  $R_1$ ,  $R_2$  and  $B_1$ ,  $B_2$ . The absorption lines  $B_1$  and  $B_2$  are located at  $\sim 21000 \text{ cm}^{-1}$  and their Zeeman effects have not been observed yet. These will be reported in the second paper (Part B).

As for the broad bands, detailed quantitative measurements, especially on splittings and anisotropies, seem absent as far as we know although Thosar<sup>4)</sup> has briefly reported the optical anisotropy of the first band (at the longer wave-length side). The results of experimental studies on these bands will be given in a later paper.

The knowledge about the ground state of ruby are provided by the recent experiments of paramagnetic resonance<sup>5)</sup>.

The present paper is devoted to the theoretical consideration which enables us to analyse the experimental facts already known and those to be reported later. Although details of the newly obtained experimental results will be given in later papers, the results that seem definite and important will be sometimes referred to, if necessary, in order to confirm the theory.

## § 2. The Crystal Structure

The crystal symmetry of ruby<sup>6)</sup> is, as well known, rhombohedral with its unit cell containing two molecules of  $\text{Al}_2\text{O}_3$ . Some of  $\text{Al}^{3+}$  ions are considered to be substituted by  $\text{Cr}^{3+}$  ions. Their nearest neighbours are six  $\text{O}^{2-}$  ions, which form a distorted octahedron around  $\text{Al}^{3+}$  or  $\text{Cr}^{3+}$  ion, which has neither inversion nor reflection symmetry ( $\sigma_v$ ) as Fig.

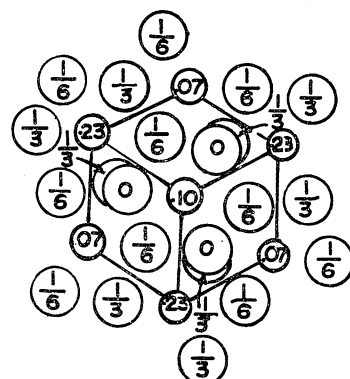


Fig. 1. A portion of the  $\text{Al}_2\text{O}_3$  arrangement projected upon a plane normal to the 3-fold axis  $C_3$  and passing through the apex of a unit rhombohedron. Fractions give distances below the projection plane measured in terms of the height of the unit rhombohedron. Atoms of Al (or Cr) are small, the oxygens are large circles. (Wyckoff, 1948)

1 shows. The symmetry of this distorted octahedron is  $C_3$  whose principal axis passes through the apexes of the unit rhombohedron. It may be noted that the four positions of  $\text{Al}^{3+}$  in the unit cell are energetically equivalent, since the four distorted octahedrons are transformed into one another by translation or both by translation and inversion at the central ion.

## § 3. The Hamiltonian for the $\text{Cr}^{3+}$ Ion and Wave Functions for $d$ -electrons

In our previous papers<sup>7)</sup> on the octahedral complexes, the effect of spin-orbit interaction has been completely neglected. For the analyses of the line spectra of ruby, the spin-orbit interaction plays an essential role together with the trigonal field as we shall see later. Thus the Hamiltonian which we must take for the  $\text{Cr}^{3+}$  ion in ruby is

$$\begin{aligned} \mathcal{H} &= \mathcal{H}_0 + \mathcal{H}' \\ \mathcal{H}' &= V_{\text{trig}} + V_{\text{s0}} \end{aligned} \quad \left. \right\}, \quad (3.1)$$

where  $\mathcal{H}_0$  is the Hamiltonian for the cubic case without spin-orbit interaction,  $V_{\text{trig}}$  the trigonal field and  $V_{s0}$  the spin-orbit interaction. Judging from the similarity of the absorption spectra of ruby to those of Cr alum, we may suppose that the cubic part will be larger than the other two terms.  $\mathcal{H}'$  will be treated as a small perturbation to the cubic system.

The eigen-functions of  $\mathcal{H}_0$  for the chromophoric electrons are already known. They are given in (3.7) of I\*, where the  $z$  axis was chosen in the direction of the fourfold axis of the octahedron. The principal axis of the trigonal field in ruby is, however, just one of the three fold axis of the octahedron, and it is

more convenient to take this axis as the axis of quantization in the present case. The cubic bases, namely, the unperturbed eigenfunctions are accordingly transformed so that they span the irreducible representations of both  $O_h$  and  $C_{3v}^{**}$ ,

$$\varphi(\Gamma M) = \sum_r \varphi(\Gamma r)(\Gamma r | \Gamma M), \quad (3.2)$$

where  $\varphi(\Gamma r)$  is the previous cubic base belonging to the  $r$  component of the cubic representation  $\Gamma$  and is abbreviated as

$$\left. \begin{array}{l} \varphi(Er) = (u, v) \\ \varphi(F_1r) = (\alpha, \beta, r)^* \\ \varphi(F_2r) = (\xi, \eta, \zeta)^* \end{array} \right\}, \quad (3.3)$$

while  $\varphi(\Gamma M)$  are abbreviated as follows:

$$\left. \begin{array}{ll} \varphi(E \pm 1) = (u_+, u_-) & \text{irreducible representation } E \text{ of } C_{3v} \\ \varphi(F_1 \pm 1) = (a_+, a_-) & E \\ \varphi(F_1 0) = a_0 & A_2 \\ \varphi(F_2 \pm 1) = (x_+, x_-) & E \\ \varphi(F_2 0) = x_0 & A_1 \end{array} \right\}. \quad (3.4)$$

These are at the same time the trigonal bases which belong to the irreducible representation of  $C_{3v}$  as shown on the right column of the above table.

The matrix elements of the unitary transformation  $(\Gamma r | \Gamma M)$  are given by

$(Er   EM)$		$(F_1r   F_1M), (F_2r   F_2M)$		
$u_+$	$u_-$	$a_+$ ( $x_+$ )	$a_-$ ( $x_-$ )	$a_0$ ( $x_0$ )
$u$	$-1/\sqrt{2}$	$1/\sqrt{2}$	$\alpha(\xi)$	$-\omega/\sqrt{3}$
$v$	$-i/\sqrt{2}$	$-i/\sqrt{2}$	$\beta(\eta)$	$-\bar{\omega}/\sqrt{3}$
			$r(\zeta)$	$-1/\sqrt{3}$

where  $\omega = e^{2\pi i/3}$  and  $\bar{\omega} = \omega^2$ .

Since almost all of the matrix elements of operators needed in this paper are already given in IV, we now proceed to the discussions of what follows from the theory.

#### § 4. Optical Anisotropy and Splitting of the Absorption Bands

As pointed out in § 1, the similarity of the absorption spectra of ruby to those of Cr alum leads us to the expectation that the absorption band at  $\sim 18000 \text{ cm}^{-1}$ , which we call  $U$  band hereafter, corresponds to the transition  $(f_2^3)^4A_2 \rightarrow (f_2^2e)^4F_2$  in the cubic case and the band

at  $\sim 25000 \text{ cm}^{-1}$  (called  $Y$  band) to the transition  $(f_2^3)^4A_2 \rightarrow (f_2^2e)^4F_1$ . This expectation will be confirmed if this assignment could explain the experimental facts<sup>8)</sup>, namely the splitting and the optical anisotropy of these bands.

Let us denote by  $U^\perp$  and  $Y^\perp$  the absorptions of  $U$  and  $Y$  when the electric vector  $E$  of the incident light is perpendicular to the optic axis  $C_3$ , and by  $U^//$  and  $Y^//$  those when  $E$  is parallel to  $C_3$ . The outline of the observed splittings and anisotropies of the bands

\* As to the choice of phase of these bases, see § 2 of IV<sup>10)</sup>.

\*\* Although actual symmetry of the field which electrons subject to is  $C_3$ , it is allowed to treat it as if  $C_{3v}$  when we deal with the crystal energy of  $d$ -electrons.

to be reported later is as follows: Each absorption peak of  $U^{\parallel\parallel}$  and  $Y^{\parallel\parallel}$  is found at the shorter wave-length side of the corresponding peak of  $U^{\perp}$  and  $Y^{\perp}$ . The splitting amounts approximately to  $500 \text{ cm}^{-1}$  for both  $U$  and  $Y$ . The absorption intensity of  $U^{\perp}$  is much higher than that of  $U^{\parallel\parallel}$  (the ratio is more than 2), while the absorption intensity of  $Y^{\perp}$  is fairly low compared to that of  $Y^{\parallel\parallel}$  (the ratio is about 1/2). The intensity of  $U^{\perp}$  is comparable to that of  $Y^{\perp}$ .

These experimental facts, especially the marked optical anisotropies of  $U$  and  $Y$  offer, as we shall see, important evidences in favour of the above assignments. The study of the optical anisotropy in the present case is as powerful as the study of the optical rotatory power. The importance of the study of the rotatory power in making the assignment of  ${}^4F_1$  and  ${}^4F_2$  has been recently emphasized by Moffitt<sup>9)</sup>.

#### (a) The splitting

Strictly speaking, we must take the spin-orbit interaction into account as well as the trigonal field, in order to discuss the splitting of the bands. Let us, however, neglect the effect of the former for a while. Then group theory shows that  ${}^4F_2$  level splits into two sublevels  ${}^4E$  and  ${}^4A_1$  of  $C_{3v}$  and  ${}^4F_1$  into  ${}^4E$  and  ${}^4A_2$  under the action of the trigonal field. If we adopt the assumption of strong field limit (i.e. neglect of the configuration interaction among the cubic levels), the positions of these split components measured from the respective unperturbed positions of  ${}^4F_2$  and  ${}^4F_1$  are given by

$$\left. \begin{aligned} f_2^2 e {}^4F_2 & \left\{ {}^4E \langle {}^4F_2 x_{\pm} | V_{\text{trig}} | {}^4F_2 x_{\pm} \rangle = K/2 \right. \\ & \left. {}^4A_1 \langle {}^4F_2 x_0 | V_{\text{trig}} | {}^4F_2 x_0 \rangle = -K \right\} \\ f_2^2 e {}^4F_1 & \left\{ {}^4E \langle {}^4F_1 a_{\pm} | V_{\text{trig}} | {}^4F_1 a_{\pm} \rangle = K/2 \right. \\ & \left. {}^4A_2 \langle {}^4F_1 a_0 | V_{\text{trig}} | {}^4F_1 a_0 \rangle = -K \right\}, \end{aligned} \right. \quad (4.1)$$

$$f_2 e {}^4F_1 \left\{ \begin{aligned} {}^4E \langle {}^4F_1 a_{\pm} | V_{\text{trig}} | {}^4F_1 a_{\pm} \rangle &= K \\ {}^4A_2 \langle {}^4F_1 a_0 | V_{\text{trig}} | {}^4F_1 a_0 \rangle &= -2K \end{aligned} \right\}, \quad (4.2)$$

in terms of a parameter  $K$  which measures the strength of the trigonal field and is related to the splitting on one electron level  $f_2$ :

$$(f_2 x_{\pm} | v_{\text{rig}} | f_2 x_{\pm}) = K, \quad (f_2 x_0 | v_{\text{trig}} | f_2 x_0) = -2K. \quad (4.2)$$

(The  $e$  level is not split by the action of trigonal field. Note also that the trigonal field as a tensor operator is of type  $F_2$  and  $V_{\text{trig}} = V_0(F_2)$  in the notation of IV<sup>10)</sup>.

Thus, as far as we neglect the interaction among the sublevels split from different cubic levels, the magnitudes of the splitting of  $f_2^2 e {}^4F_2$  and  $f_2^2 e {}^4F_1$  are both  $3K/2$ .  ${}^4A_1$  and  ${}^4A_2$  sublevels are on the shorter wave-length side of each  ${}^4E$  sublevels, in case  $K$  is negative, and *vice versa*. As will be seen in the next subsection, the present case seems to be just the former one, and we have

$$K \sim -350 \text{ cm}^{-1} \quad (4.3)$$

from the observed splitting. This value of  $K$  in turn justifies the neglect of the effect of spin-orbit interaction in discussing the splitting of  ${}^4F_2$  and  ${}^4F_1$ , since the order of magnitude of the relevant matrix elements of  $V_{s0}$  will be that of the spin orbit coupling parameter  $\lambda = \zeta/3$  which will be at most as large as  $\sim 90 \text{ cm}^{-1}$  (see § 5).

#### (b) The optical anisotropy

In the case of octahedral complex ions, all electric dipole transitions between the multiplets  $f_2^n e^n S\Gamma_g$  were forbidden at the equilibrium configuration of nuclei because of the presence of centre of symmetry and the observed intensities of the absorption bands of these ions have been explained by taking the vibrational distortion of the octahedron into account.

In contrast, the environment of  $\text{Cr}^{3+}$  ion in ruby has no centre of symmetry. The naturally unsymmetrical field (the hemihedral part of the trigonal field  $V_{\text{hem}}$ ) will make the electric dipole transition slightly allowed even in the absence of vibrational distortion. Although the effect of the latter might not be quite negligible, we will discard it in the discussion of the optical anisotropy and concern ourselves only with the effect of the former. This is also somewhat justified by the experimental facts to be reported later that the dependence of the oscillator strength of the absorption bands on temperature is slight at relatively high temperatures and that the band shapes vary with temperature roughly in the same way as that of allowed transitions.

The dipole strength of the transition between the ground state  ${}^4A_2$  and the component  $M$  of the excited state  ${}^4\Gamma_g$  is the square of the absolute value of the following matrix element:

$$\begin{aligned} & ({}^4A_{2g} | \overline{P} | {}^4\Gamma_g M) \\ &= \sum_{\Gamma_u' M'} \frac{({}^4A_{2g} | P | {}^4\Gamma_u' M') ({}^4\Gamma_u' M' | V_{\text{hem}} | {}^4\Gamma_g M)}{W({}^4\Gamma_g) - W({}^4\Gamma_u')} \end{aligned}$$

$$+ \sum_{P_u' M'} \frac{(^4A_{2g}|V_{\text{hem}}| ^4\Gamma_u' M') (^4\Gamma_u' M' |P| ^4\Gamma_g M)}{W(^4A_{2g}) - W(^4\Gamma_u')} , \quad (4.4)$$

where  $^4\Gamma_u'$  is the higher excited state with odd parity and  $W(^4\Gamma_u')$  is the energy of that state.  $P$  is the electric dipole moment vector  $\sum e r_i$  of the system,  $P = (P_x, P_y, P_z)$ . It is more convenient to use the following linear combination of  $P_x$  and  $P_y$  corresponding to the present choice of bases,

$$\left. \begin{aligned} P_+ &= -\frac{1}{\sqrt{2}}(P_x + iP_y), \\ P_- &= \frac{1}{\sqrt{2}}(P_x - iP_y), \\ P_0 &= P_z, \end{aligned} \right\} \quad (4.5)$$

so that

$$\left. \begin{aligned} P &= -P_- k^+ - P_+ k^- + P_0 k^0, \\ k^+ &= -\frac{1}{\sqrt{2}}(i + ij), \\ k^- &= \frac{1}{\sqrt{2}}(i - ij), \\ k^0 &= k, \\ |k^+|^2 = |k^-|^2 &= \frac{1}{2}(i^2 + j^2), \end{aligned} \right\} \quad (4.6)$$

where  $i, j$  and  $k$  are the unit vectors in the directions of  $x, y$  and  $z$  coordinate axes respectively.

$V_{\text{hem}}$  must be invariant under the trigonal rotation, and changes sign under the inversion with respect to the origin. If it is expanded in powers of the coordinates of electrons, the first term which will be predominant is of the form  $\kappa \sum_i z_i$ . This term is of type  $F_{1u}$  as an irreducible tensor operator and will be denoted as  $V_0(F_{1u})$  in the following. If we assume  $V_{\text{hem}} = V_0(F_{1u})$ , the excited state  $^4\Gamma_u'$  in (4.4) is restricted to  $^4F_{2u}$ , since  $P$  is also an operator of the type  $F_{1u}$ . Then we find

$$\left. \begin{aligned} (^4A_2 | \bar{P} | ^4F_{2u} \pm ) &= \pm \frac{i}{\sqrt{2}} \cdot \alpha (^4A_2 \rightarrow ^4F_2) \cdot k^\pm, \\ (^4A_2 | \bar{P} | ^4F_{2u} 0 ) &= 0, \end{aligned} \right\} \quad (4.7)$$

$$\left. \begin{aligned} (^4A_2 | \bar{P} | ^4F_{1u} \pm ) &= -\frac{1}{\sqrt{6}} \cdot \alpha (^4A_2 \rightarrow ^4F_1) \cdot k^\pm, \\ (^4A_2 | \bar{P} | ^4F_{1u} 0 ) &= \frac{\sqrt{2}}{\sqrt{3}} \cdot \alpha (^4A_2 \rightarrow ^4F_1) \cdot k^0, \end{aligned} \right\} \quad (4.8)$$

where  $\alpha$ 's are suitable proportionality factors

which can be evaluated from (4.4), and the corresponding dipole strengths are

$$\left. \begin{aligned} W(^4A_2 \rightarrow ^4F_2 : ^4E) &= \sum_{M=x_+, x_-} W(^4A_2 \rightarrow ^4F_2 M) \\ &\propto \frac{1}{2} |\alpha (^4A_2 \rightarrow ^4F_2)|^2 \cdot (i^2 + j^2), \\ W(^4A_2 \rightarrow ^4F_2 : ^4A_2) &= W(^4A_2 \rightarrow ^4F_2 0) = 0, \end{aligned} \right\} \quad (4.9)$$

$$\left. \begin{aligned} W(^4A_2 \rightarrow ^4F_1 : ^4E) &= \sum_{M=a_+, a_-} W(^4A_2 \rightarrow ^4F_1 M) \\ &\propto \frac{1}{6} |\alpha (^4A_2 \rightarrow ^4F_1)|^2 \cdot (i^2 + j^2), \\ W(^4A_1 \rightarrow ^4F_1 : ^4A_1) &= W(^4A_2 \rightarrow ^4F_1 0) \\ &\propto \frac{2}{3} |\alpha (^4A_2 \rightarrow ^4F_1)|^2 k^2. \end{aligned} \right\} \quad (4.10)$$

The transition probabilities for the linearly polarized light  $E//C_3$  are given by the coefficients of  $k^2$  and those the linearly polarized light  $E \perp C_3$  by the coefficients of  $i^2$  or  $j^2$  in (4.9) and (4.10). Thus with the assignments

$$\left. \begin{aligned} U^{II} : f_2^3 | ^4A_{2g} \rightarrow (f_2^2 e) ^4F_{2g} : ^4A_1 \\ U^\perp : \quad \quad \quad \rightarrow (f_2^2 e) ^4F_{2g} : ^4E \\ Y^{II} : \quad \quad \quad \rightarrow (f_2^2 e) ^4F_{1g} : ^4A_2 \\ Y^\perp : \quad \quad \quad \rightarrow (f_2^2 e) ^4F_{1g} : ^4E \end{aligned} \right\} \quad (4.11)$$

we have the following ratios between the dipole strengths;

$$\left. \begin{aligned} \omega(U^{II}) : \omega(U^\perp) &= 0 : 1 \\ \omega(Y^{II}) : \omega(Y^\perp) &= 4 : 1 \end{aligned} \right\}. \quad (4.12)$$

Although the result are not quite satisfactory, the present simple treatment seems to explain the qualitative feature of the observed optical anisotropy in each absorption band under a reasonable assumption. The causes of the discrepancy between the theory and experiment may be as follows; the assumption  $V_{\text{hem}} = V_0(F_{1u})^*$  and the neglect of the vibrational effect. We need, however, more detailed knowledge of the trigonal field and the vibrations excited in the crystal in order to improve the results. These problems will be left for future investigations, together with the unexplained ratio of the absorption intensities of  $U$  to that of  $Y$ .

## § 5. Splitting and Optical Anisotropy of the Absorption Lines

For the absorption lines  $R_1$  and  $R_2$  of ruby,

\* Note that (4.7) and (4.8) holds as long as we assume  $V_{\text{hem}}$  is of type  $F_{1u}$ . They were derived by consideration solely based on the transformation properties of operators and wave functions.

we expect the assignments  $f_2^3 A_2 \rightarrow$  split components of  $f_2^3 E$  or  $f_2^3 F_1$ , and for  $B_1$  and  $B_2$   $f_2^3 A_2 \rightarrow$  split components of  $f_2^3 F_2$ , just as in the case of Cr alum. In this section, we will discuss the splitting of  $f_2^3: ^2E$ ,  $^2F_2$  and  $^2F_1$  levels due to the action of the trigonal field and the spin-orbit interaction, and also the optical anisotropy of the absorption lines corresponding to the transition to these split components from the ground state.

### (a) The splitting

As pointed out in IV, the splitting of  $^2E$  is described by the effective Hamiltonian

$$\mathcal{H}_{\text{eff}} = \lambda S_z T(A_2), \quad (5.1)$$

where  $\lambda$  is a parameter to be determined empirically and  $T(A_2)$  is an orbital operator whose matrix representation is

$$\begin{matrix} u_+ & \left| \begin{array}{cc} 1 & \\ & -1 \end{array} \right| \\ u_- & \end{matrix}. \quad (5.2)$$

The eigenvalues of the above Hamiltonian and the corresponding eigenfunctions are

$$W_1 = \frac{1}{2}\lambda \quad 2\bar{A}^* \begin{cases} \Psi(^2E, \frac{1}{2}, u_+)^* \\ \Psi(^2E, -\frac{1}{2}, u_-)^* \end{cases} \quad (5.3)$$

$$W_2 = -\frac{1}{2}\lambda \quad \bar{E}^* \begin{cases} \Psi(^2E, -\frac{1}{2}, u_+) \\ \Psi(^2E, \frac{1}{2}, u_-) \end{cases} \quad (5.4)$$

It remains to express the parameter  $\lambda$  in terms of known matrix elements. This is easy if we confine ourselves to the second order perturbation in  $\mathcal{H}'$ . Since  $^2E$  does not split by the sole action of the trigonal field or of the spin orbit interaction, but split only through the interplay of these two, it follows

$$\begin{aligned} & (^2EM_s M | \mathcal{H}_{\text{eff}} | ^2EM_s M) \\ &= \sum_{s' M' M} \frac{1}{W(^2E) - W(^2I')} \\ &\quad \times \{ (^2EM_s M | V_{\text{trig}} | ^2\Gamma M_s' M') \\ &\quad \cdot (^2\Gamma M_s' M' | V_{so} | ^2EM_s M) \\ &\quad + \text{complex conjugate} \}. \end{aligned} \quad (5.5)$$

If the intermediate states  $^2I'$  are restricted to those in configuration  $f_2^3$  that makes a large contribution in the above summation, the summation reduces to a single term with  $^2\Gamma = ^2F_2$ , since  $^2E$  does not couple with  $^2F_1$  either through the trigonal field or the spin-orbit interaction. To make the following discussion

clear, the coupling scheme among the doublets in configuration  $f_2^3$  and the quartets in configuration  $f_2^2 e$  are illustrated in Fig. 2. Eva-

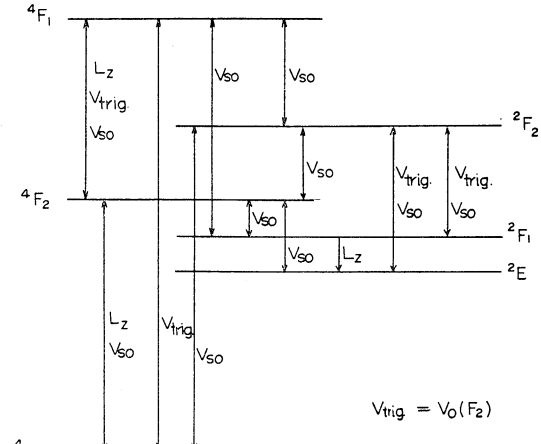


Fig. 2. The coupling scheme among the doublets  $^2E$ ,  $^2F_2$  and  $^2F_1$  in configuration  $f_2^3$  and the quartets  $^4A_2(f_2^3)$ ,  $^4F_2(f_2^2e)$  and  $^4F_1(f_2^2e)$ .

luating the matrix elements in (5.5) with the aid of the tables given in the Appendix and comparing (5.5) with (5.1), we find

$$\lambda(^2E) = 4K\zeta / \{W(^2E) - W(^2F_2)\} \quad (5.6)$$

where  $\zeta$  is defined by

$$\zeta = -2(f_2, \frac{1}{2}, x_+ | v_{so} | f_2, \frac{1}{2}, x_+), \quad (5.7)$$

while  $\zeta'$  which appears in the following discussion is defined by

$$\zeta' = -\sqrt{2}(f_2, \frac{1}{2}, x_+ | v_{so} | e, \frac{1}{2}, u_+), \quad (5.8)$$

in which  $v_{so} = \zeta s \cdot l$ . In this section we assume that  $\zeta$  and  $\zeta'$  are isotropic. The second order terms which come from  $V_{\text{trig}}^2$  and  $V_{so}^2$  cause only a shift of  $^2E$  as a whole.

The effective Hamiltonian for  $^2F_2$  is of the form:

$$\mathcal{H}_{\text{eff}} = FV_0 + \lambda(S_x T_x + S_y T_y) + \lambda_0 S_z T_z, \quad (5.9)$$

where  $V_0$  and  $T_x$ ,  $T_y$ ,  $T_z$  are the operators whose matrix representations are given respectively by

$$\begin{matrix} & x_+ & x_- & x_0 \\ & -1 & & \\ V_0: x_+ & \parallel & & \\ x_- & & -1 & \\ & & & \\ x_0 & \parallel & & 2 \end{matrix}$$

\* These are the two-valued representations of  $C_3$ .

\*\*  $\frac{1}{2}$  denotes the spin quantum number  $M_s$ .

$$T_x: \begin{array}{c} x_+ \\ x_- \\ x_0 \end{array} \left\| \begin{array}{ccc} & x_+ & x_- \\ & -1/\sqrt{2} & -1/\sqrt{2} \\ -1/\sqrt{2} & -1/\sqrt{2} & 0 \end{array} \right\| \begin{array}{c} x_+ \\ x_- \\ x_0 \end{array} \left\| \begin{array}{ccc} & x & x_- \\ & -i/\sqrt{2} & i/\sqrt{2} \\ -i/\sqrt{2} & i/\sqrt{2} & 0 \end{array} \right\| \begin{array}{c} x_+ \\ x_- \\ x_0 \end{array} \left\| \begin{array}{ccc} & x_+ & x_- \\ & i/\sqrt{2} & -i/\sqrt{2} \\ -i/\sqrt{2} & i/\sqrt{2} & 0 \end{array} \right\| \begin{array}{c} x_+ \\ x_- \\ x_0 \end{array} \left\| \begin{array}{ccc} & -1 & 1 \\ & 1 & 0 \end{array} \right\|. \quad (5.10)$$

The eigenvalues of (5.9) and the corresponding eigenfunctions are

$$W_0 = -F - \frac{\lambda_0}{2} \quad 2\bar{A} \begin{cases} \Psi(^2F_2, \frac{1}{2}, x_+) \\ \Psi(^2F_2, -\frac{1}{2}, x_-) \end{cases} \quad (5.11)$$

$$W_1 = -F + \frac{\lambda_0}{2} - \frac{\lambda}{\sqrt{2}} \tan \alpha \quad \bar{E}_a \begin{cases} \Psi(^2F_2, -\frac{1}{2}, x_+) \cos \alpha + \Psi(^2F_2, \frac{1}{2}, x_0) \sin \alpha \\ \Psi(^2F_2, \frac{1}{2}, x_-) \cos \alpha + \Psi(^2F_2, -\frac{1}{2}, x_0) \sin \alpha \end{cases} \quad (5.12)$$

$$W_2 = -F + \frac{\lambda_0}{2} + \frac{\lambda}{\sqrt{2}} \cot \alpha \quad \bar{E}_b \begin{cases} \Psi(^2F_2, \frac{1}{2}, x_0) \cos \alpha - \Psi(^2F_2, -\frac{1}{2}, x_+) \sin \alpha \\ \Psi(^2F_2, -\frac{1}{2}, x_0) \cos \alpha - \Psi(^2F_2, \frac{1}{2}, x_-) \sin \alpha \end{cases}, \quad (5.13)$$

where

$$\tan 2\alpha = \sqrt{2}\lambda / \left( 3F - \frac{\lambda_0}{2} \right), \quad 0 \leq \alpha \leq \frac{\pi}{2}. \quad (5.14)$$

$F$ ,  $\lambda$  and  $\lambda_0$  can also be expressed in terms of  $K$  and  $\zeta$ . Let us first consider  $F$ . Since  $(f_2^{3^2} F_2 M_s M | V_{\text{trig}} | f_2^{3^2} F_2 M_s M)$  vanishes, trigonal field splits  ${}^2F_2$  through the second order perturbation:

$$\sum_{\Gamma M'} \frac{1}{W({}^2F_2) - W(\Gamma)} ({}^2F_2 M_s M | V_{\text{trig}} | {}^2\Gamma M_s M') ({}^2\Gamma M_s M' | V_{\text{trig}} | {}^2F_2 M_s M). \quad (5.15)$$

This, however, causes the shift of  ${}^2F_2$  as a whole as well as the splitting. The magnitude of the shift is equal to the trace of the above expression divided by 6. Subtracting this from (5.15) and comparing suitable matrix element of the resulting expression with the corresponding element of the first term of (5.9), we find under the same assumption as before

$$F({}^2F_2) = -2K^2 / \{W({}^2F_2) - W({}^2E)\} - K^2 / \{W({}^2F_2) - W({}^2F_1)\}. \quad (5.16)$$

$(f_2^{3^2} F_2 M_s M | V_{s0} | f_2^{3^2} F_2 M'_s M')$  also vanishes and the second and the third term in (5.9) come from the second order perturbation:

$$\sum_{\Gamma M''} \frac{1}{W({}^2F_2) - W(\Gamma)} \{ ({}^2F_2 M_s M | V_{\text{trig}} | {}^2\Gamma M_s M'') ({}^2\Gamma M_s M'' | V_{s0} | {}^2F_2 M'_s M') + \text{c.c.} \}. \quad (5.17)$$

Proceeding as before we obtain

$$\begin{aligned} \lambda({}^2F_2) &= 2K\zeta / \{W({}^2F_2) - W({}^2E)\} + K\zeta / \{W({}^2F_2) - W({}^2F_1)\}, \\ \lambda_0({}^2F_2) &= -4K\zeta / \{W({}^2F_2) - W({}^2E)\} - 2K\zeta / \{W({}^2F_2) - W({}^2F_1)\}, \end{aligned} \quad \} \quad (5.18)$$

where the contributions from the second order term  $V_{s0}^2$  are neglected, since they are estimated to be negligible if we use the value of  $\zeta$  to be determined later.

The effective Hamiltonian for  ${}^2F_1$  is of the same form as that for  ${}^2F_2$ . The matrix elements of the operator  $T$  for  $F_1$  state is just the opposite sign (negative) of the corresponding elements for  $F_2$  though those of  $V_0$  are same for both  $F_1$  and  $F_2$ . The eigen-values and the eigenfunctions for  ${}^2F_1$  is thus written

down at once by changing the sign of  $\lambda$ ,  $\lambda_0$  and writting  ${}^2F_1 a_+$  etc. for  ${}^2F_2 x_+$  etc. in (5.11)~(5.14).  $F$ ,  $\lambda$  and  $\lambda_0$  in this case are expressed in terms of  $K$  and  $\zeta$  in the following way:

$$F({}^2F_1) = -K^2 / \{W({}^2F_1) - W({}^2F_2)\}, \quad (5.19)$$

$$\begin{aligned} \lambda({}^2F_1) &= -K\zeta / \{W({}^2F_1) - W({}^2F_2)\}, \\ \lambda_0({}^2F_1) &= 2K\zeta / \{W({}^2F_1) - W({}^2F_2)\}, \end{aligned} \quad \} \quad (5.20)$$

in which the second order terms  $V_{s0}^2$  are again neglected.

We will now discuss the splittings of the

doublets in greater detail.

$^2E$  splits into two Kramers doublets  $2\bar{A}(^2E)$  and  $\bar{E}(^2E)$ . Here  $2\bar{A}$  lies on the shorter wavelength side if  $\lambda(^2E) > 0$ . This is really the case since it was found in § 4 that  $K$  is negative. Further considerations on the anisotropy and the Zeeman effect of the characteristic doublet  $R_1$  and  $R_2$  establish the following assignments in agreement with this prediction:

$$\begin{aligned} R_1(14418 \text{ cm}^{-1}): & ^4A_2 \rightarrow \bar{E}(^2E) \\ R_2(14447 \text{ cm}^{-1}): & ^4A_2 \rightarrow 2\bar{A}(^2E) \end{aligned} \quad \} . \quad (5.21)$$

Using the observed splitting  $\lambda(^2E) \sim 30 \text{ cm}^{-1}$  and taking  $W(^2E) - W(^2F_2)$  to be  $\sim -6500 \text{ cm}^{-1}$ , the magnitude of  $\zeta$  is found to be  $\sim 140 \text{ cm}^{-1}$ . This is fairly small compared to the free-ion value  $\sim 270 \text{ cm}^{-1}$  adopted by Owen<sup>11</sup>, but not unreasonably small in view of the fact that the value of  $\zeta$  generally decreases in crystals.

With this value of  $\zeta$ , the approximate values of  $F$ ,  $\lambda$  and  $\lambda_0$  can now be estimated for  $^2F_2$  and  $^2F_1$  using (5.16), (5.18) and (5.19), (5.20) respectively:

$$\begin{aligned} F(^2F_2) &\sim -60 \text{ cm}^{-1} \\ \lambda_0(^2F_2) &\sim +45 \text{ cm}^{-1} \\ \lambda(^2F_2) &\sim -22 \text{ cm}^{-1} \end{aligned} \quad \} , \quad (5.22)$$

$$\begin{aligned} F(^2F_1) &\sim +20 \text{ cm}^{-1} \\ \lambda_0(^2F_1) &\sim +15 \text{ cm}^{-1} \\ \lambda(^2F_1) &\sim -8 \text{ cm}^{-1} \end{aligned} \quad \} , \quad (5.23)$$

and for these values,

$$\alpha(^2F_2) \sim 0, \quad \alpha(^2F_1) \sim 0,$$

where it was assumed that  $W(^2F_2) - W(^2E) \approx W(^2F_2) - W(^2F_1)$ . The predicted arrangements of the split components of  $^2F_2$  and  $^2F_1$  are

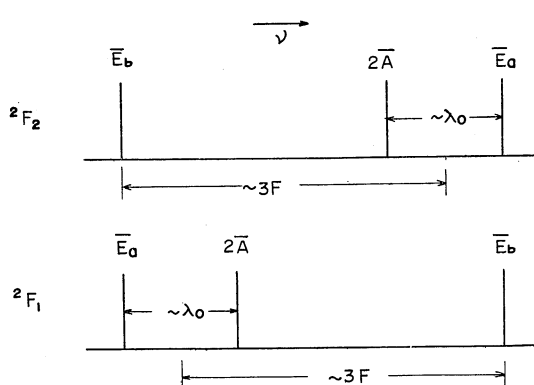


Fig. 3. The splittings of  $^2F_2$  and  $^2F_1$ .

given in Fig. 3. The lines that correspond to the transitions to the split components of  $^2F_1$  are not yet identified. As to those of  $^2F_2$  it is fairly certain, as will be seen in the following, that the following assignments can be made for  $B_1$  and  $B_2$ :

$$\begin{aligned} B_1(20993 \text{ cm}^{-1}): & ^4A_2 \rightarrow 2\bar{A}(^2F_2) \\ B_2(21068 \text{ cm}^{-1}): & ^4A_2 \rightarrow \bar{E}_a(^2F_2) \end{aligned} \quad \} . \quad (5.24)$$

If  $\alpha(^2F_2) \sim 0$ , we have  $\lambda_0 \sim 75 \text{ cm}^{-1}$  from the observed separation of  $B_1$  and  $B_2$ .

As far as we are concerned with the split components  $2\bar{A}$  and  $\bar{E}_a$  the predicted arrangement is qualitatively good\*, but quantitatively not quite satisfactory (compare the experimental value of  $\lambda_0$  with  $\lambda_0$  in (5.22)). This disagreement is perhaps partly due to the omission of the interaction between  $^2F_2$  and any higher excited doublet which will be larger for  $^2F_2$  than for the deeply lying  $^2E$ , and partly due to the assumption  $W(^2F_2) - W(^2E) \approx W(^2F_2) - W(^2F_1)$ . Though the position of  $^2F_1$  has not been known yet, it is highly probable that  $^2F_1$  has a higher energy than that of  $^2E$  judging from the sign and the magnitude of the  $g$ -shifts of the split components  $2\bar{A}(^2E)$  and  $\bar{E}(^2E)$  (§ 6 (e)). This will increase the theoretical value of  $\lambda_0(^2F_2)$ .

#### (b) The optical anisotropy

We assume as in II that the intensities of the line absorption are borrowed from those of the absorption bands through the spin-orbit interaction, that is, the dipole strength for the transition from the component  $a$  of the ground state  $^4A_2$  to the component  $b$  of the doublet  $^2F$  is given by the square of the matrix element

$$\begin{aligned} & (^4A_2a | \bar{P} | ^2F b) \\ & = \sum (^4A_2a | \bar{P} | ^4F' c) (^4F' c | V_{s0} | ^2F b) \\ & / \{ W(^2F) - W(^4F') \} , \end{aligned} \quad (5.25)$$

where  $c$  is the components of the excited quartets  $^4F_2$  and  $^4F_1$ . This means that the contamination of the doublet states to the

\* Though the arrangement of  $2\bar{A}(^2F_2)$  and  $\bar{E}_a(^2F_2)$  is qualitatively good, we cannot observe any absorption line at the long wave-length side of them. Somewhat broad line can be observed at the shorter wave-length side ( $21357 \text{ cm}^{-1}$  at  $78^\circ\text{K}$ )<sup>2</sup>. Thus, our theory might be wrong even qualitatively with respect to the predicted position of  $\bar{E}_b(^2F_2)$ .

ground quartet is neglected\*.

Using the tables of the Appendix, the dipole strengths evaluated by the formula (5.25) are given in Tables I and II, with  $\alpha=0$  in (5.12, 5.13).  $\pi$ 's and  $\sigma$ 's are expressed in terms of  $\zeta'$  and the dipole strengths of the bands. Using the abbreviations,

$$\begin{aligned} \mathbf{P}_\alpha^0, \pm(U) &= ({}^4A_2|\bar{\mathbf{P}}_\alpha|^4F_2x_{0,\pm}) \\ \mathbf{P}_\alpha^0, \pm(Y) &= ({}^4A_2|\bar{\mathbf{P}}_\alpha|^4F_1a_{0,\pm}) \end{aligned} \quad \left. \right\}, \quad (5.26)$$

they are expressed as follows; for the components of  ${}^2F_2$

$$\begin{aligned} \pi_\alpha &= \frac{4}{3} \zeta'^2 \left| \frac{\mathbf{P}_\alpha^0(U)}{W({}^2E) - W({}^4F_2)} \right|^2, \\ \sigma_{\pm\alpha} &= \frac{4}{3} \zeta'^2 \left| \frac{\mathbf{P}_\alpha^\pm(U)}{W({}^2E) - W({}^4F_2)} \right|^2, \end{aligned} \quad \left. \right\} \quad (5.27)$$

and for  ${}^2F_2$

Table I. The values of  $|({}^4A_2M_s|\bar{\mathbf{P}}|^2EM_s', M')|^2$ , in which  $M_s$  is quantized with respect to the  $z$  axis.

${}^4A_2$	$M_s$	${}^2E$	$2\bar{A}$	$\bar{E}$	
		$M_s', M'$	$1/2, u_+$	$-1/2, u_-$	$-1/2, u_+$
	3/2	$\pi_\alpha/2$			$\sigma_{+\alpha}/2$
	1/2	$\sigma_{+\alpha}/3$	$\sigma_{+\alpha}/6$	$\pi_\alpha/6$	$\sigma_{-\alpha}/3$
	-1/2	$\sigma_{-\alpha}/6$	$\sigma_{-\alpha}/3$	$\sigma_{+\alpha}/3$	$\sigma_{-\alpha}/3$
	-3/2	$\pi_\alpha/2$	$\sigma_{-\alpha}/2$	$\pi_\alpha/2$	$\sigma_{-\alpha}/2$

Table II. The values of  $|({}^4A_2M_s|\bar{\mathbf{P}}|^2F_2M_s', M')|^2$  and  $|({}^4A_2M_s|\bar{\mathbf{P}}|^2F_1M_s', M')|^2$ , in which  $M_s$  is quantized with respect to the  $z$  axis.

${}^4A_2$	$M_s$	${}^2F_2({}^2F_1)$	$2\bar{A}$	$\bar{E}_a$	$\bar{E}_b$		
		$M_s', M'$	$-1/2, x_+(a_+)$	$1/2, x_-(a_-)$	$-1/2, x_+(a_+)$	$1/2, x_-(a_-)$	$1/2, x_0(a_0)$
	3/2	$\pi_\alpha/2$			$\sigma_{+\alpha}^0/2$	$\sigma'_{+\alpha}/2$	
	1/2	$\sigma_{+\alpha}/3$	$\sigma_{+\alpha}^0/6$	$\pi_\alpha/6$	$\sigma_{-\alpha}/3$	$\pi_\alpha'/3$	$\sigma'_{-\alpha}/6$
	-1/2	$\sigma_{-\alpha}^0/6$	$\sigma_{-\alpha}/3$	$\sigma_{+\alpha}/3$	$\pi_\alpha/6$	$\sigma'_{+\alpha}/6$	$\pi_\alpha'/3$
	-3/2	$\pi_\alpha/2$	$\sigma_{-\alpha}/2$	$\sigma_{-\alpha}^0/2$			$\sigma'_{+\alpha}/2$
		$\pi_\alpha = \frac{1}{2} \zeta'^2 \left\{ \left  \frac{\mathbf{P}_\alpha^0(U)}{W({}^2F_2) - W({}^4F_2)} \right ^2 + \left  \frac{\mathbf{P}_\alpha^0(Y)}{W({}^2F_2) - W({}^4F_1)} \right ^2 \right\},$					
		$\sigma_{\pm\alpha} = \frac{1}{2} \zeta'^2 \left  \frac{\mathbf{P}_\alpha^\pm(U)}{W({}^2F_2) - W({}^4F_2)} \pm i \frac{\mathbf{P}_\alpha^\pm(Y)}{W({}^2F_2) - W({}^4F_1)} \right ^2,$					
		$\sigma_{\pm 0} = 2\zeta'^2 \left  \frac{\mathbf{P}_\alpha^\pm(Y)}{W({}^2F_2) - W({}^4F_1)} \right ^2,$					
		$\pi_{\alpha'} = 2\zeta'^2 \left  \frac{\mathbf{P}_\alpha^0(Y)}{W({}^2F_2) - W({}^4F_1)} \right ^2,$					
		$\sigma'_{\pm\alpha} = \frac{1}{2} \zeta'^2 \left  \frac{\mathbf{P}_\alpha^\pm(U)}{W({}^2F_2) - W({}^4F_2)} \mp i \frac{\mathbf{P}_\alpha^\pm(Y)}{W({}^2F_2) - W({}^4F_1)} \right ^2,$					

$$\left. \begin{aligned} \pi_\alpha &= \frac{1}{6} \zeta'^2 \left\{ \left| \frac{\mathbf{P}_\alpha^0(U)}{W({}^2F_1) - W({}^4F_2)} \right|^2 + 9 \left| \frac{\mathbf{P}_\alpha^0(Y)}{W({}^2F_1) - W({}^4F_1)} \right|^2 \right\}, \\ \sigma_{\pm\alpha} &= \frac{1}{6} \zeta'^2 \left| \frac{\mathbf{P}_\alpha^\pm(U)}{W({}^2F_1) - W({}^4F_2)} \mp i \frac{3\mathbf{P}_\alpha^\pm(Y)}{W({}^2F_1) - W({}^4F_1)} \right|^2, \\ \sigma_{\pm 0} &= \frac{2}{3} \zeta'^2 \left| \frac{\mathbf{P}_\alpha^\pm(U)}{W({}^2F_1) - W({}^4F_2)} \right|^2, \\ \pi_{\alpha'} &= \frac{2}{3} \zeta'^2 \left| \frac{\mathbf{P}_\alpha^0(U)}{W({}^2F_1) - W({}^4F_2)} \right|^2, \\ \sigma'_{\pm\alpha} &= \frac{1}{6} \zeta'^2 \left| \frac{\mathbf{P}_\alpha^\pm(U)}{W({}^2F_1) - W({}^4F_2)} \pm i \frac{3\mathbf{P}_\alpha^\pm(Y)}{W({}^2F_1) - W({}^4F_1)} \right|^2, \end{aligned} \right\} \quad (5.29)$$

and for  ${}^2F_1$

$$\left. \begin{aligned} \pi_\alpha &= \frac{1}{6} \zeta'^2 \left\{ \left| \frac{\mathbf{P}_\alpha^0(U)}{W({}^2F_1) - W({}^4F_2)} \right|^2 + 9 \left| \frac{\mathbf{P}_\alpha^0(Y)}{W({}^2F_1) - W({}^4F_1)} \right|^2 \right\}, \\ \sigma_{\pm\alpha} &= \frac{1}{6} \zeta'^2 \left| \frac{\mathbf{P}_\alpha^\pm(U)}{W({}^2F_1) - W({}^4F_2)} \mp i \frac{3\mathbf{P}_\alpha^\pm(Y)}{W({}^2F_1) - W({}^4F_1)} \right|^2, \\ \sigma_{\pm 0} &= \frac{2}{3} \zeta'^2 \left| \frac{\mathbf{P}_\alpha^\pm(U)}{W({}^2F_1) - W({}^4F_2)} \right|^2, \\ \pi_{\alpha'} &= \frac{2}{3} \zeta'^2 \left| \frac{\mathbf{P}_\alpha^0(U)}{W({}^2F_1) - W({}^4F_2)} \right|^2, \\ \sigma'_{\pm\alpha} &= \frac{1}{6} \zeta'^2 \left| \frac{\mathbf{P}_\alpha^\pm(U)}{W({}^2F_1) - W({}^4F_2)} \pm i \frac{3\mathbf{P}_\alpha^\pm(Y)}{W({}^2F_1) - W({}^4F_1)} \right|^2, \end{aligned} \right\} \quad (5.29)$$

\* Note that  ${}^4F_2$  and  ${}^4F_1$  hybridize with the neighbouring doublets  ${}^2E$ ,  ${}^2F_1$  and  ${}^2F_2$  to a larger extent than that  ${}^2F_2$  does with the ground quartet. Note also that  ${}^2F_2$  is the only one among the doublets that couples with the ground state.

where  $\alpha=z$  and  $\alpha=x$  for  $E//C_3$  and  $E\perp C_3$  respectively.

Then we observe that, for the sum of the strengths of the split components,  $\Sigma_\alpha$ , the following expressions should be given:

$$\Sigma_\alpha(^2E) = \frac{4}{3}\{\pi_\alpha + (\sigma_{+\alpha} + \sigma_{-\alpha})\} = \frac{16}{9}\zeta'^2 \sum_{k=0,+,-} \left| \frac{\mathbf{P}_{\alpha^k}(U)}{W(^2E) - W(^4F_2)} \right|^2, \quad (5.30)$$

$$\begin{aligned} \Sigma_\alpha(^2F_2) &= \frac{2}{3}\{2\pi_\alpha + \pi'_\alpha + (\sigma_{+\alpha} + \sigma_{-\alpha}) + (\sigma'_{+\alpha} + \sigma'_{-\alpha}) + (\sigma^0_{+\alpha} + \sigma^0_{-\alpha})\} \\ &= \frac{2}{3}\zeta'^2 \sum_{k=0,+,-} \left| \frac{\mathbf{P}_{\alpha^k}(U)}{W(^2F_2) - W(^4F_2)} \right|^2 + 2\zeta'^2 \sum_{k=0,+,-} \left| \frac{\mathbf{P}_{\alpha^k}(Y)}{W(^2F_2) - W(^4F_1)} \right|^2, \end{aligned} \quad (5.31)$$

$$\begin{aligned} \Sigma_\alpha(^2F_1) &= \frac{2}{3}\{2\pi_\alpha + \pi'_\alpha + (\sigma_{+\alpha} + \sigma_{-\alpha}) + (\sigma'_{+\alpha} + \sigma'_{-\alpha}) + (\sigma^0_{+\alpha} + \sigma^0_{-\alpha})\} \\ &= \frac{2}{3}\zeta'^2 \sum_{k=0,+,-} \left| \frac{\mathbf{P}_{\alpha^k}(U)}{W(^2F_1) - W(^4F_2)} \right|^2 + 2\zeta'^2 \sum_{k=0,+,-} \left| \frac{\mathbf{P}_{\alpha^k}(Y)}{W(^2F_1) - W(^4F_1)} \right|^2. \end{aligned} \quad (5.32)$$

The relative magnitude of these quantities can thus be estimated from the observed relative strengths of the bands.

If we could neglect the effect of the vibrationally allowed part of transitions, we have

$$\pi_x = \pi'_x = \sigma_{\pm z} = \sigma'_{\pm z} = \sigma^0_{\pm z} = 0, \quad (5.33)$$

and

$$\left. \begin{array}{l} \sigma_{+x} = \sigma_{-x} \equiv \sigma, \\ \sigma'_{+x} = \sigma'_{-x} \equiv \sigma', \\ \sigma^0_{+x} = \sigma^0_{-x} \equiv \sigma^0, \end{array} \right\} \quad (5.34)$$

since for the real trigonal field

$$(\mathbf{P}_x^\pm)^* = -\mathbf{P}_x^\mp. \quad (5.35)$$

Thus it becomes possible to predict several relations among the intensities of the split components. Using the parameters  $\sigma$ ,  $\sigma^0$ ,  $\pi = \pi_z$  and  $\pi' = \pi'_z$ , the calculated intensities are given in Table III. Comparing these with

Table III. The calculated absorption intensities of the line spectra corresponding to transitions to the split components of  $^2E$ ,  $^2F_2$  and  $^2F_1$ .

	$E \perp C_3$	$E//C_3$
$^2E$	$2\bar{A}$	$\sigma$
	$\bar{E}$	$5\sigma/3$
$^2F_2$ or $^2F_1$	$2\bar{A}$	$2\sigma/3 + \sigma_0/3$
	$\bar{E}_a$	$2\sigma/3 + \sigma_0$
	$\bar{E}_b$	$4\sigma'/3$
		$2\pi'/3$

the experimental results given in Fig. 1 of Part B, we shall see that the assignments given in subsection (a) explain nicely the observed intensity ratios between  $R_1^{\perp, //}$  and  $R_2^{\perp, //}$  and between  $B_1^{\perp, //}$  and  $B_2^{\perp, //}$  (the superscripts denote the polarization). In order to

explain the ratios between  $B_1^{\perp, //}$  and  $B_2^{\perp, //}$ ,  $R_1^{\perp, //}$  and  $R_2^{\perp, //}$  it is necessary to know the relations among the parameters  $\sigma$ ,  $\sigma^0$ ,  $\pi$  and  $\pi'$ . It will be shown in Part B that if we assume the relations  $\sigma \sim 2\pi$  for  $^2E$  and  $\sigma^0 \sim 2\sigma$ ,  $\pi \sim 3\sigma$  for  $^2F_2$ , all the above-mentioned intensity ratios observed are explained.

We notice that for  $B_1$  the absorption is stronger in the case  $E//C_3$  than in the case  $E\perp C_3$  while for  $R_2$  the relation is reversed. This can be easily understood since  $B_1(B_2)$  borrows most of its intensity from  $Y$  band which shows a strong absorption for the light  $E//C_3$  while  $R_1(R_2)$  borrows all of its intensity from  $U$  band whose anisotropy is reverse to that of  $Y$  band.

If the transitions corresponding to  $U$  and  $Y$  bands are assumed to be allowed only by the hemihedral part of trigonal field and the relation  $\sigma \sim \sigma'$  is assumed to be approximately valid, we can use the observed anisotropy of these bands to get the relations among the parameters  $\sigma$ ,  $\sigma^0$ ,  $\pi$  and  $\pi'$ . Putting

$$\omega(U^{\perp, //}) : \omega(U^{\perp, //}) : \omega(Y^{\perp, //}) : \omega(Y^{\perp, //}) = 1 : 3 : 3 : 6$$

to give approximately the observed anisotropy of the bands, we obtain the relations  $\sigma \sim 1.5\pi$  for  $^2E$  and  $\sigma^0 \sim 4\sigma$ ,  $\pi \sim 2\sigma$  for  $^2F_2$ . This should be compared to the above mentioned empirical relations. The agreement is fair.

We will next see to what extent the relation (5.30) is satisfied. Inserting the observed intensity ratios of  $R$ 's absorptions,  $\omega(R_1^{\perp, //}) : \omega(R_1^{\perp, //}) : \omega(R_2^{\perp, //}) : \omega(R_2^{\perp, //}) = 10 : 2 : 7 : 4$ , we obtain  $\Sigma_z(^2E) / \Sigma_z(^2E) = 6/17 \approx 1/3$  which nicely agrees with the observed anisotropy of  $U$  band,  $\omega(U^{\perp, //}) / \omega(U^{\perp, //}) = 1/3$ .

$\bar{E}_b(^2F_2)$  is yet unidentified. The line that will

correspond to this level will show marked anisotropy, because using the observed anisotropy of  $U$  and  $Y$  bands the relation  $\pi' \sim 4\pi$  can be derived and so together with the empirical relation  $\pi \sim 3\sigma$  (the approximate relation  $\sigma \sim \sigma'$  is also assumed here as before) we suppose that the parallel component will be six times stronger than the perpendicular component. The strength of the parallel component of the line corresponding to  $\bar{E}_a(^2F_2)$  thus calculated becomes more than twice that of  $B_1$ .

The lines that will correspond to the components of  $^2F_1$  borrow their intensities almost equally from both  $U$  and  $Y$  bands if they are located near  $R_1$  and  $R_2$ . The expected anisotropy of these lines (corresponding to  $\bar{E}_a(^2F_1)$  and  $2\bar{A}(^2F_1)$ ) are somewhat similar to that of  $R_1$  and  $R_2$  and there is a possibility that  $R_1$  and  $R_2$  correspond respectively to  $\bar{E}_a(^2F_1)$  and  $2\bar{A}(^2F_1)$ . This possibility is, however, excluded by the consideration of the Zeeman effect which will be discussed in the following section.

## § 6. Zeeman Effect of the Absorption Lines

### (a) Zeeman splitting of the excited states

For the discussion of the Zeeman effect of  $^2E$ , we use the following simplified effective Hamiltonian:

$$\begin{aligned} \mathcal{H}_{\text{eff}} = & \lambda S_z T(A_2) + g_{//} \beta H_{0z} S_z \\ & + g_{\perp} \beta (H_{0x} S_x + H_{0y} S_y) \\ & + (g_{//}' \beta H_{0z} + g_{\perp}' \beta H_{0x} + g_{\perp}' \beta H_{0y}) T(A_2), \end{aligned} \quad (6.1)$$

neglecting the term of  $\beta \mathbf{H}_0 \cdot \mathbf{g} \cdot \mathbf{S} \cdot \mathbf{V}(E)$  in (3.2) of IV, which is negligible in the present case.

The splitting factor  $g^*$  for  $2\bar{A}(^2E)$  and  $\bar{E}(^2E)$

\* The sign of the  $g_{//}$ -values of the split components are defined in the following way: The states correspond to the wave functions of the upper (lower) lines of (5.3), (5.4), (5.11), (5.12) and (5.13) have Zeeman energy  $\frac{1}{2}g_{//}\beta H_0(-\frac{1}{2}g_{//}\beta H_0)$ . The negative sign taken for  $g_{//}(\bar{E}_a)$  might be queer at the first sight. It is, however, natural if we notice that, in the present case,  $\bar{M}=M_s+M$  is the quantum number for the state  $\Psi(^2F, M_s, M)$  and we take the definition of the  $g_{//}$  factor, Zeeman energy =  $g_{//}\beta \bar{M} H_0$ , just as in the case of the Zeeman effect of free atoms.

Simple consideration based on the selection rule shows that this negative  $g_{//}(\bar{E})$  value is the cause of the appearance of the side component of  $R_1$  when  $E//C_3$  ( $4\bar{M} \equiv 0, \text{ mod } 3$ )  $H_0/C_3$  and the strong central component when  $E \perp C_3$  ( $4\bar{M} \equiv \pm 1, \text{ mod } 3$ ).

when  $H_0//C_3$  is readily found as

$$\left. \begin{aligned} g_{//}(2\bar{A}) &= g_{//} + 2g_{//}', \\ g_{//}(\bar{E}) &= -(g_{//} - 2g_{//}'), \end{aligned} \right\} \quad (6.2)$$

When  $H_0 \perp C_3$ , it is also found that

$$\left. \begin{aligned} g_{\perp}(2\bar{A}) &= 2g_{\perp}', \\ g_{\perp}(\bar{E}) &= 2g_{\perp}', \end{aligned} \right\} \quad (6.3)$$

and a magnetic field causes the shifts of  $2\bar{A}$  and  $\bar{E}$  as follows;

$$\left. \begin{aligned} \text{for } 2\bar{A}(^2E) & \quad \beta^2 H^2 / \lambda(^2E), \\ \text{for } \bar{E}(^2E) & \quad -\beta^2 H^2 / \lambda(^2E), \end{aligned} \right\} \quad (6.4)$$

but this is negligible if  $\lambda(^2E)$  is very large compared to the Zeeman energy just as in the present case.

The orbital angular momentum is quenched in  $^2E$  and the first order correction in  $g_{//}$ ,  $g_{//}'$  and  $g_{\perp}'$  vanishes, namely

$$\sum_{^2F} \left\{ \frac{(^2E|L+2S|^2\Gamma)(^2\Gamma|\mathcal{H}'|^2E)}{W(^2E)-W(^2I)} + \text{c.c.} \right\} = 0, \quad (6.5)$$

as long as intermediate doublets are limited to those of  $f_2^3$  (see Fig. 2). We thus expect

$$\left. \begin{aligned} g_{//}(2\bar{A}) &\doteq 2, & g_{\perp}(2\bar{A}) &\doteq 0, \\ g_{//}(\bar{E}) &\doteq -2, & g_{\perp}(\bar{E}) &\doteq 0. \end{aligned} \right\} \quad (6.6)$$

For  $^2F_2$  and  $^2F_1$ , we take the Hamiltonian,

$$\begin{aligned} \mathcal{H}_{\text{eff}} = & g_{//} \beta H_{0z} S_z + g_{\perp} \beta (H_{0x} S_x + H_{0y} S_y) \\ & + g_{//}' \beta H_{0z} T_z + g_{\perp}' \beta (H_{0x} T_x + H_{0y} T_y). \end{aligned} \quad (6.7)$$

We find then for the components of  $^2F_2$

$$\left. \begin{aligned} g_{//}(2\bar{A}) &= g_{//} - 2g_{//}', \\ g_{//}(\bar{E}_a) &= -(g_{//} \cos 2\alpha + 2g_{//}' \cos^2 \alpha), \\ g_{//}(\bar{E}_b) &= g_{//} \cos 2\alpha - 2g_{//}' \sin^2 \alpha, \end{aligned} \right\} \quad (6.8)$$

and of  $^2F_1$

$$\left. \begin{aligned} g_{//}(2\bar{A}) &= g_{//} + 2g_{//}', \\ g_{//}(\bar{E}_a) &= -(g_{//} \cos \alpha - 2g_{//}' \cos^2 \alpha), \\ g_{//}(\bar{E}_b) &= g_{//} \cos \alpha + 2g_{//}' \sin^2 \alpha. \end{aligned} \right\} \quad (6.9)$$

When  $H_0 \perp C_3$ , assuming large initial splitting of the components, we find for  $^2F_2$

$$\left. \begin{aligned} g_{\perp}(2\bar{A}) &= 0, \\ |g_{\perp}(\bar{E}_a)| &= |g_{\perp} \sin^2 \alpha - \sqrt{2} g_{\perp}' \sin 2\alpha|, \\ |g_{\perp}(\bar{E}_b)| &= |g_{\perp} \cos^2 \alpha + \sqrt{2} g_{\perp}' \sin 2\alpha|. \end{aligned} \right\} \quad (6.10)$$

and for  $^2F_1$

$$\left. \begin{aligned} g_{\perp}(2\bar{A}) &= 0, \\ |g_{\perp}(\bar{E}_a)| &= |g_{\perp} \sin^2 \alpha + \sqrt{2} g_{\perp}' \sin 2\alpha|, \\ |g_{\perp}(\bar{E}_b)| &= |g_{\perp} \cos^2 \alpha - \sqrt{2} g_{\perp}' \sin 2\alpha|. \end{aligned} \right\} \quad (6.11)$$

The first order correction in  $g_{//}$ ,  $g_{//}'$  and  $g_{\perp}'$  vanishes also in this case, and we obtain  $g_{//} = 2$ ,  $g_{\perp} = 2$  (spin part) and  $g_{//}' = 1$ ,  $g_{\perp}' = 1$  (orbital part). Thus we get, assuming  $\alpha = 0$ , for  $^2F_2$

$$\left. \begin{aligned} g_{//}(2\bar{A}) &= 0, & g_{\perp}(2\bar{A}) &= 0, \\ g_{//}(\bar{E}_a) &= -4, & g_{\perp}(\bar{E}_a) &= 0, \\ g_{//}(\bar{E}_b) &= 2, & |g_{\perp}(\bar{E}_b)| &= 2, \end{aligned} \right\} \quad (6.12)$$

for  $^2F_1$

$$\left. \begin{aligned} \Psi(M_s^{(x)} = \pm \frac{3}{2}) &= \frac{1}{2\sqrt{2}} \left\{ \pm \Psi(M_s^{(z)} = \frac{3}{2}) + \Psi(M_s^{(z)} = -\frac{3}{2}) \right\} \\ &\quad + \frac{\sqrt{-3}}{2\sqrt{2}} \left\{ \Psi(M_s^{(z)} = \frac{1}{2}) \pm \Psi(M_s^{(z)} = -\frac{1}{2}) \right\}, \\ \Psi(M_s^{(x)} = \pm \frac{1}{2}) &= \frac{\sqrt{-3}}{2\sqrt{2}} \left\{ \mp \Psi(M_s^{(z)} = \frac{3}{2}) + \Psi(M_s^{(z)} = -\frac{3}{2}) \right\} \\ &\quad - \frac{1}{2\sqrt{2}} \left\{ \Psi(M_s^{(z)} = \frac{1}{2}) \mp \Psi(M_s^{(z)} = -\frac{1}{2}) \right\}. \end{aligned} \right\} \quad (6.14)$$

Table IV. The Values of  $\sum_{M_s, M'} |(^4A_2 M_s | \bar{P} |^2 E M_s', M')|^2$ , in which  $M_s$  is quantized with respect to the  $x$  axis.

$^4A_2$	$M_s$	$2\bar{E}$	$2\bar{A}$	$\bar{E}$
	3/2	$\pi_\alpha/8 + 3(\sigma_{+\alpha} + \sigma_{-\alpha})/16$		$\pi_\alpha/8 + 3(\sigma_{+\alpha} + \sigma_{-\alpha})/16$
	1/2	$3\pi_\alpha/8 + (\sigma_{+\alpha} + \sigma_{-\alpha})/16$		$\pi_\alpha/24 + 11(\sigma_{+\alpha} + \sigma_{-\alpha})/48$
	-1/2	$3\pi_\alpha/8 + (\sigma_{+\alpha} + \sigma_{-\alpha})/16$		$\pi_\alpha/24 + 11(\sigma_{+\alpha} + \sigma_{-\alpha})/48$
	-3/2	$\pi_\alpha/8 + 3(\sigma_{+\alpha} + \sigma_{-\alpha})/16$		$\pi_\alpha/8 + 3(\sigma_{+\alpha} + \sigma_{-\alpha})/16$

Table V. The tables of  $\sum_{M_s, M'} |(^4A_2 M_s | \bar{P} |^2 F_2 M_s', M')|^2$  and  $\sum_{M_s, M'} |(^4A_2 M_s | \bar{P} |^2 F_1 M_s', M')|^2$ , in which  $M_s$  is quantized with respect to the  $x$  axis.

$^4A_2$	$M_s$	$2F_2(2F_1)$	$2\bar{A}$	$\bar{E}_a$
	3/2	$\pi_\alpha/8 + (\sigma_{+\alpha} + \sigma_{-\alpha})/8 + (\sigma_{+\alpha}^0 + \sigma_{-\alpha}^0)/16$		$\pi_\alpha/8 + (\sigma_{+\alpha} + \sigma_{-\alpha})/8 + (\sigma_{+\alpha}^0 + \sigma_{-\alpha}^0)/16$
	1/2	$3\pi_\alpha/8 + (\sigma_{+\alpha} + \sigma_{-\alpha})/24 + (\sigma_{+\alpha}^0 + \sigma_{-\alpha}^0)/48$		$\pi_\alpha/24 + (\sigma_{+\alpha} + \sigma_{-\alpha})/24 + 3(\sigma_{+\alpha}^0 + \sigma_{-\alpha}^0)/16$
	-1/2	$3\pi_\alpha/8 + (\sigma_{+\alpha} + \sigma_{-\alpha})/24 + (\sigma_{+\alpha}^0 + \sigma_{-\alpha}^0)/48$		$\pi_\alpha/24 + (\sigma_{+\alpha} + \sigma_{-\alpha})/24 + 3(\sigma_{+\alpha}^0 + \sigma_{-\alpha}^0)/16$
	-3/2	$\pi_\alpha/8 + (\sigma_{+\alpha} + \sigma_{-\alpha})/8 + (\sigma_{+\alpha}^0 + \sigma_{-\alpha}^0)/16$		$\pi_\alpha/8 + (\sigma_{+\alpha} + \sigma_{-\alpha})/8 + (\sigma_{+\alpha}^0 + \sigma_{-\alpha}^0)/16$

Using (6.14) the strengths of the Zeeman components in this case can be derived also from Tables I and II, they are given in Tables IV and V. In the predicted Zeeman patterns (Figs. 4, 5), the absence of the vibrational ef-

fect is assumed, i.e.,  $\pi_x = \pi'_x = \sigma_{\pm z} = \sigma_{\pm z}^0 = \sigma'_{\pm z} = 0$ .

### (c) Zeeman splitting of the ground state

The Zeeman levels of the ground state have been well examined by paramagnetic reso-

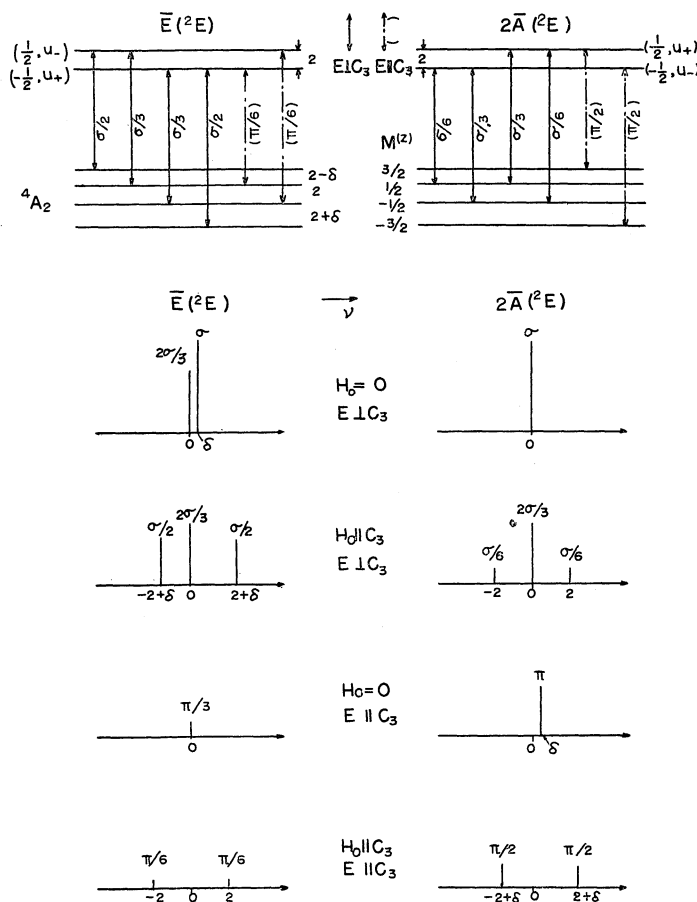


Fig. 4 (a). The predicted Zeeman patterns ( $H_0||C_3$ ) for  ${}^2E$ . Splittings are given in  $\beta H_0$  unit.

nance. To analyse optical Zeeman patterns, the knowledge about them is also necessary, so that we shall summarize it below: The energies of the split components of the ground quartet are

$$\left. \begin{aligned} W(M_s^{(\omega)} = \pm \frac{3}{2}) &= \pm \frac{3}{2}g_{0\parallel}\beta H_0, \\ W(M_s^{(\omega)} = \pm \frac{1}{2}) &= \pm \frac{1}{2}g_{0\parallel}\beta H_0 + \delta, \end{aligned} \right\} \quad (6.15)$$

when  $H_0 \perp C_3$  and

$$\left. \begin{aligned} W(M_s^{(\omega)} = \pm \frac{3}{2}) &= \pm \frac{3}{2}g_{0\perp}\beta H_0 + \frac{\delta}{4}, \\ W(M_s^{(\omega)} = \pm \frac{1}{2}) &= -\frac{1}{2}g_{0\perp}\beta H_0 + \frac{3\delta}{4}, \end{aligned} \right\} \quad (6.16)$$

when  $H_0 \parallel C_3$  ( $2\beta H_0 \gg \delta$ ).

The paramagnetic resonance experiment has shown that

$$|\delta| = 0.38 \text{ cm}^{-1}, \quad g_{0\parallel} \doteq g_{0\perp} \doteq 2.$$

#### (d) The Zeeman patterns

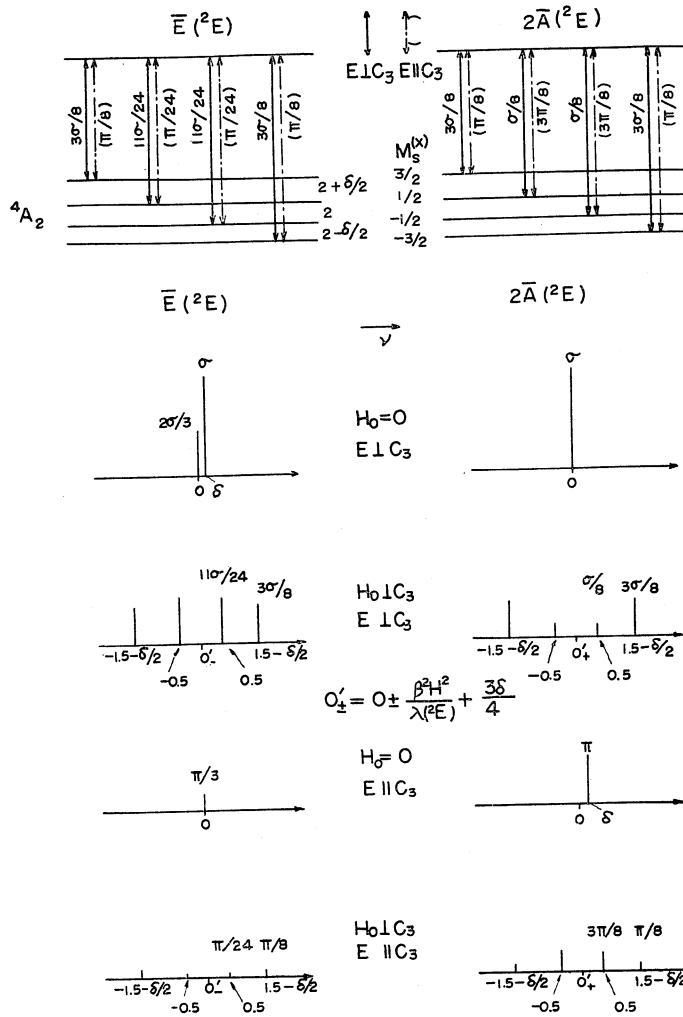
Now we are ready to predict the Zeeman patterns, and they are illustrated in Figs. 4 and 5. From the detailed comparison of these patterns with the experimental ones that will be made in Part B, we may conclude that the assignments (5.21) for  $R_1$  and  $R_2$  and (5.24) for  $B_1$  and  $B_2$  are established.

Moreover, from such comparison, we find that  $\delta$  is positive and the  $g$ -values of the split components of  ${}^2E$  and  ${}^2F_2$  show fairly large shift from those expected in (6.6) and (6.12).

#### (e) $g$ -shifts of the excited states

The observed  $g_{\parallel}$ -shifts of the split components of  ${}^2E$  are

$$\left. \begin{aligned} g_{\parallel}(2\bar{A}) &\doteq 2-2A, \\ |g_{\parallel}(\bar{E})| &\doteq 2+2A, \\ A &\doteq 0.2. \end{aligned} \right\} \quad (6.17)$$

Fig. 4 (b). The predicted Zeeman patterns ( $H_0 \perp C_3$ ).

These relations show that in (6.3)  $g_{//}'$  deviates from zero and  $g_{//}' = -0.2$ . Such a large deviation seems curious at first glance.

In order to explain the cause of such shifts, we must consider the second order effect in  $\mathcal{H}'$ . Group theoretical consideration shows

$$\begin{aligned}
 g_{//}' &= \{(^2E, \frac{1}{2}, u_+ | L_z |^2 F_1, \frac{1}{2}, a_+) (^2F_1, \frac{1}{2}, a_+ | V_{\text{trig}} |^2 F_2, \frac{1}{2}, x_+) (^2F_2, \frac{1}{2}, x_+ | V_{\text{trig}} |^2 E, \frac{1}{2}, u_+) + \text{c.c.}\} \\
 &\quad / \{W(^2E) - W(^2F_1)\} \{W(^2E) - W(^2F_2)\} \\
 &+ \{(^2E, \frac{1}{2}, u_+ | V_{\text{trig}} |^2 F_2, \frac{1}{2}, x_+) (^2F_2, \frac{1}{2}, x_+ | L_z |^2 F_2, \frac{1}{2}, x_+) (^2F_2, \frac{1}{2}, x_+ | V_{\text{trig}} |^2 E, \frac{1}{2}, u_+) \\
 &\quad / \{W(^2E) - W(^2F_2)\}^2 \\
 &+ \{(^2E, \frac{1}{2}, u_+ | V_{\text{trig}} |^2 F_2, \frac{1}{2}, x_+) (^2F_2, \frac{1}{2}, x_+ | 2S_z |^2 F_2, \frac{1}{2}, x_+) (^2F_2, \frac{1}{2}, x_+ | V_{s0} |^2 E, \frac{1}{2}, u_+) + \text{c.c.}\} \\
 &\quad / \{W(^2E) - W(^2F_2)\}^2 \\
 &- \frac{1}{2} \{(^2E, \frac{1}{2}, u_+ | V_{\text{trig}} |^2 F_2, \frac{1}{2}, x_+) (^2F_2, \frac{1}{2}, x_+ | V_{s0} |^2 E, \frac{1}{2}, u_+) + \text{c.c.}\} \{(^2E, \frac{1}{2}, u_+ | 2S_z |^2 E, \frac{1}{2}, u_+)\} \\
 &\quad / \{W(^2E) - W(^2F_2)\}^2
 \end{aligned} \tag{6.18}$$

that the operator of type  $T(A_2)$  can be found only in the reduction of the products of operators  $L_z \times V_{\text{trig}} \times V_{\text{trig}}$  and  $S_z \times V_{\text{trig}} \times V_{s0}$  into their irreducible parts. Hence we have (see Fig. 2)

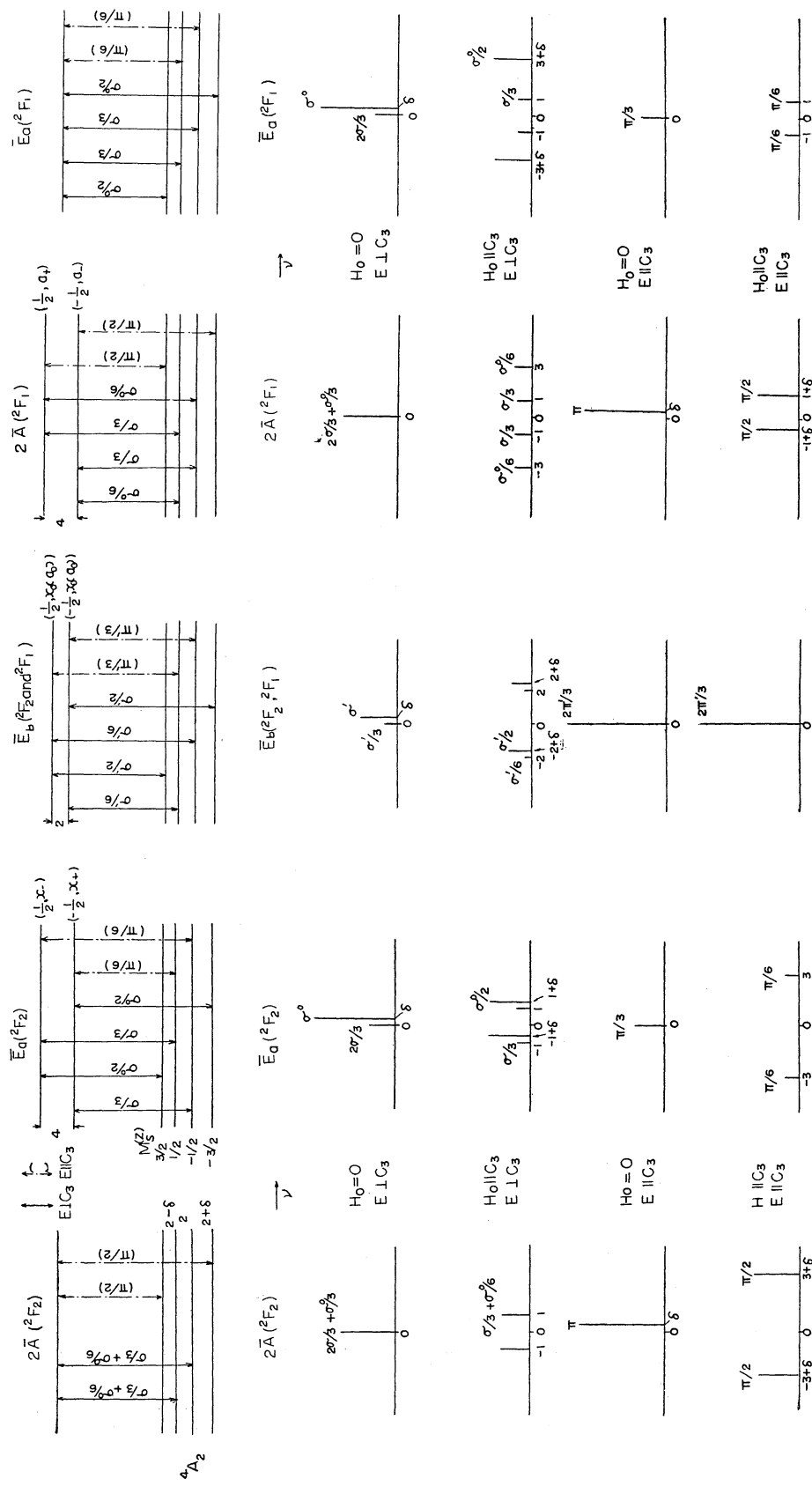
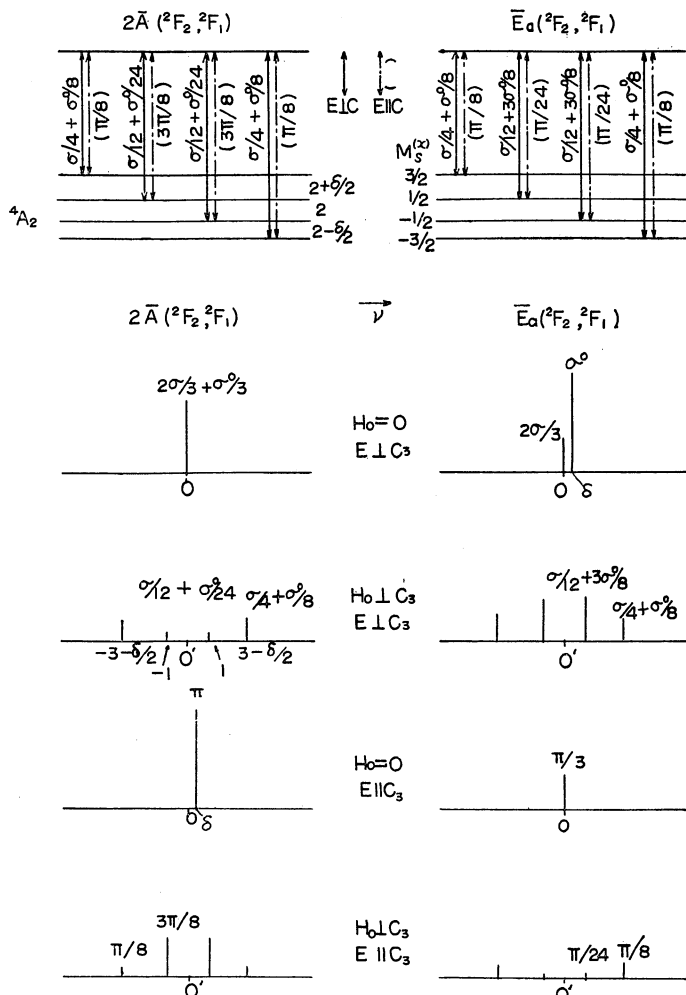


Fig. S5 (a). The predicted Zeeman patterns ( $H_0 || C_3$ ).

Fig. 5 (b). The predicted Zeeman patterns ( $H_0 \perp C_3$ ).

The terms on the last three lines cancel out, and we have

$$g_{//}(^2E) = -12K^2/(W(^2E) - W(^2F_1))(W(^2E) - W(^2F_2)) - 6K^2/(W(^2E) - W(^2F_2))^2. \quad (6.19)$$

The second term is fairly small (if  $K \sim -350 \text{ cm}^{-1}$ ,  $W(^2E) - W(^2F_2) \sim -6500 \text{ cm}^{-1}$ , it becomes  $\sim -0.02$ ), but the first term will make a large contribution, since  $^2F_1$  is supposed to be near  $^2E$ . If we estimate the separation of these levels from the above formula, using the empirical value of  $g_{//}(^2E) \doteq -0.2$ ,

$$W(^2E) - W(^2F_1) \doteq -1200 \text{ cm}^{-1}, \quad (6.20)$$

which is a reasonable value for this separation and we expect from this that the energy of  $^2F_1$  is higher than that of  $^2E$ .

Similar consideration shows that the deviation of  $g_{//}(^2E)$  from  $2, 4g_{//}(^2E)$ , also comes mainly from the second order correction (also see Fig. 2);

$$\begin{aligned} 4g_{//}(^2E) &= 2(^2E, \frac{1}{2}, u_+ | L_z | ^2 F_1, \frac{1}{2}, a_+) (^2F_1, \frac{1}{2}, a_+ | V_{s0} | ^2 F_2, \frac{1}{2}, x_+) (^2F_2, \frac{1}{2}, x_+ | V_{\text{trig}} | ^2 E, \frac{1}{2}, u_+) + \text{c.c.} \\ &\quad / (W(^2E) - W(^2F_1))(W(^2E) - W(^2F_2)) \\ &\quad + 2(^2E, \frac{1}{2}, u_+ | V_{s0} | ^2 F_2, \frac{1}{2}, x_+) (^2F_2, \frac{1}{2}, x_+ | V_{\text{trig}} | ^2 F_1, \frac{1}{2}, a_+) + \text{c.c.} \\ &\quad \cdot (^2F_1, \frac{1}{2}, a_+ | L_z | ^2 E, \frac{1}{2}, u_+) / (W(^2E) - W(^2F_1))(W(^2E) - W(^2F_2)) \\ &= -8\zeta K / (W(^2E) - W(^2F_1))(W(^2E) - W(^2F_2)), \end{aligned} \quad (6.21)$$

which is estimated as  $\sim 0.05$ , using the values  $\zeta \sim 140 \text{ cm}^{-1}$  and (6.20). Such a small value of  $4g_{\parallel}/(^2E)$  also justifies the use of the simplified Hamiltonian (6.1), because the neglected terms are found to be of the order of magnitude of this deviation  $4g_{\parallel}/(^2E)$  multiplied by  $\beta H_0$ .

It must be remarked that a large deviation of  $g_{\parallel}/(^2E)$  and a small  $g_{\parallel}/(^2E)$ -shift are due to the special situation,  $V_{\text{trig}} > V_{s0}$ , in our problem.

By the same reasoning we might expect the deviation of  $g_{\parallel}/(^2F_1)$  to be of the same order of magnitude as that for  $g_{\parallel}/(^2E)$  while  $g$ -values for  $^2F_2$  are fairly close to those given in (6.12), since any crystal level cannot be expected to lie near  $^2F_2$  as close as  $^2F_1$  does to  $^2E$ . Such an expectation, however, is betrayed by the experimental results (Part B § 5),

$$g_{\parallel}/(2\bar{A}) \doteq 2A', \quad |g_{\parallel}/(\bar{E}_a)| \doteq 4 - 2A', \quad A' \doteq 0.4, \quad (6.22)$$

where the deviations of  $g_{\parallel}$ 's from those given in (6.12) are large. Therefore we must examine another cause of such a large deviation for  $^2F_2$ .

In  $^2F_2$ , (also in  $^2F_1$ ), orbital angular momentum is not quenched and it gives finite value of  $g_{\parallel}/$  in (6.8) and (6.9);

$$\begin{aligned} g_{\parallel}/ &= (F_1a_+|L_z|F_1a_+) = -(F_1a_-|L_z|F_1a_-) \\ &= (F_2x_-|L_z|F_2x_-) = -(F_2x_+|L_z|F_2x_+) \\ &= k, \end{aligned} \quad (6.23)$$

where  $k$  is defined as

$$k \equiv (f_2x_-|L_z|f_2x_-) = -(f_2x_+|L_z|f_2x_+). \quad (6.24)$$

If  $f_2$ -orbital is constructed from pure  $d$ -orbitals,  $k$  is equal to 1 and we have (6.12) and (6.13), but if we are allowed to suppose that  $f_2$ -orbital is deformed by making a covalent bonding with the surroundings and accordingly is not of pure  $d$ -character,  $k$  is not necessarily equal to 1. Thus, in place of  $g_{\parallel}$ 's in (6.12) and (6.13), we have for  $^2F_2$

$$\left. \begin{aligned} g_{\parallel}/(2\bar{A}) &\doteq 2(1-k), \\ g_{\parallel}/(\bar{E}_a) &\doteq -2(1+k), \\ g_{\parallel}/(\bar{E}_b) &\doteq 2. \end{aligned} \right\} \quad (6.25)$$

and for  $^2F_1$

$$\left. \begin{aligned} g_{\parallel}/(2\bar{A}) &\doteq 2(1+k), \\ g_{\parallel}/(\bar{E}_a) &\doteq -2(1-k), \\ g_{\parallel}/(\bar{E}_b) &\doteq 2. \end{aligned} \right\} \quad (6.26)$$

To satisfy the empirical relations (6.22), we must choose

$$k \doteq 0.6. \quad (6.27)$$

In  $^2E$  the orbital angular momentum is quenched but it contributes to  $g_{\parallel}/(^2E)$  and  $4g_{\parallel}/(^2E)$  through higher order correction of type  $L_z V_{\text{trig}}^2$ . Thus the right hand side of (6.19) and (6.21) must be multiplied also by  $k$ . Then (6.20) becomes

$$W(^2E) - W(^2F_1) \doteq 700 \text{ cm}^{-1}. \quad (6.20')$$

## § 7. Connection to the Paramagnetic Resonance Absorption

The analysis of the optical absorption spectra affords important informations not only on the excited electronic states but also on the ground state. For instance, the analyses of the Zeeman effect of the line spectra (Part B § 4) and the polarization-shift (Part B § 3 (d)) show that, of the two Kramers doublets  $M_s = \pm 3/2$  and  $M_s = \pm 1/2$  of the ground quartet  $^4A_2$ ,  $M_s = \pm 3/2$  is the lower, and lead to the following value for the natural splitting

$$\delta = W(\pm 1/2) - W(\pm 3/2) = 0.36 \pm 0.03 \text{ cm}^{-1}. \quad (7.1)$$

This value should be compared with the following precise value determined by the method of paramagnetic resonance absorption

$$|\delta| = 0.38 \text{ cm}^{-1}. \quad (7.2)$$

It should be noted, however, that this method gives us only the absolute value of  $\delta$ , whereas the optical absorption could determine the sign as well as the approximate value.

Since detailed knowledges of the excited states are now in our hands, we can go a little further and examine whether this value of  $\delta$  is consistent or not with the other empirical values determined here.

It will then be noticed that the sign of  $\delta$  is inconsistent with the sign of  $K$  if one accepts the usual theory of the natural splitting, which leads to the following formula for  $\delta$

$$\delta = \frac{4}{3} \zeta'^2 K / \{W(^4A_2) - W(^4F_2)\}^2. \quad (7.3)$$

This formula is, however, derived under the assumption of isotropic spin-orbit interaction, and is not adequate for the present case, because the  $g$ -value of the ground quartet obtained by the paramagnetic resonance absorption shows the anisotropy<sup>5)</sup>, namely

$$\left. \begin{aligned} \Delta g_{0\parallel} &= -g_{0\parallel} + 2.0023 = 0.0183 \pm 0.0006 \\ \Delta g_{0\perp} &= -g_{0\perp} + 2.0023 = 0.0156 \pm 0.0006 \end{aligned} \right\} \quad (7.4)$$

and this should be understood as the indication of the anisotropy in the spin-orbit interaction which has been assumed to be isotropic in the present paper.

The anisotropy of  $g$ -value is correlated with the anisotropy of the spin-orbit coupling parameter  $\zeta'$  in the following way:

$$\left. \begin{aligned} \Delta g_{0//} &= \frac{8}{3} k' \zeta_{//}' / \{ W(^4F_2) - W(^4A_2) \}, \\ \Delta g_{0\perp} &= \frac{8}{3} k' \zeta_{\perp}' / \{ W(^4F_2) - W(^4A_2) \}, \end{aligned} \right\} \quad (7.5)$$

where  $k'$  is a parameter to describe the de-

$$\begin{aligned} W(M_s) = & \sum_{M_s', M'} \frac{(^4A_2 M_s | V_{s0} | ^4F_2 M_s' M') (^4F_2 M_s' M' | V_{s0} | ^4A_2 M_s)}{W(^4A_2) - W(^4F_2)} \\ & + \sum_{M_s', M'} \frac{(^4A_2 M_s | V_{s0} | ^4F_2 M_s' M') (^4F_2 M_s' M' | V_{\text{trig}} | ^4F_2 M_s' M') (^4F_2 M_s' M' | V_{s0} | ^4A_2 M_s)}{\{ W(^4A_2) - W(^4F_2) \)^2} \\ & + \sum_{M_s', M'} \frac{(^4A_2 M_s | V_{\text{trig}} | ^4F_1 M_s a_0) (^4F_1 M_s a_0 | V_{s0} | ^4F_2 M_s' M') (^4F_2 M_s' M' | V_{s0} | ^4A_2 M_s)}{\{ W(^4A_2) - W(^4F_1) \} \{ W(^4A_2) - W(^4F_2) \}} + \text{c.c.} \quad (7.8) \end{aligned}$$

Taking the difference  $W(\pm 1/2) - W(\pm 3/2)$ , we find after evaluating relevant matrix elements

$$\begin{aligned} \delta &= \frac{8}{9} (\zeta_{//}'^2 - \zeta_{\perp}'^2) / \{ W(^4F_2) - W(^4A_2) \} + \frac{4}{9} (2\zeta_{//}'^2 + \zeta_{\perp}'^2) K / \{ W(^4F_2) - W(^4A_2) \}^2 \\ &\quad - 2\sqrt{\frac{2}{3}} K' \times \frac{4}{9} (2\zeta_{//} \zeta_{//}' + \zeta_{\perp} \zeta_{\perp}') / \{ W(^4F_2) - W(^4A_2) \} \{ W(^4F_1) - W(^4A_2) \}, \end{aligned} \quad (7.9)$$

where  $K' = -1/\sqrt{2} (f_2 x_{\pm} | v_{\text{trig}} | e u_{\pm})$ .  $K' = K$  if  $f_2$  and  $e$  are  $d$ -functions and  $v_{\text{trig}} \propto 3z^2 - r^2$ . The second term in the above expression corresponds to (7.3) and gives a negative contribution to  $\delta$  but we find that this is almost cancelled out by the third term which has been overlooked by Van Vleck<sup>12)</sup>, if we estimate the third term assuming  $K' = K$ ,  $\zeta_{//} = \zeta_{//}'$  and  $\zeta_{\perp} = \zeta_{\perp}'$ . The first term which is positive ( $\zeta_{//}' > \zeta_{\perp}'$ ) in the present case, gives  $\delta$  with the positive sign,

$$\delta \approx 0.3 \sim 0.6, \quad (7.10)$$

if we take  $k' = k = 0.6$ , which is a reasonable value. The values of  $\zeta'$ 's are accordingly

$$\left. \begin{aligned} \zeta_{//}' &\sim 200 \\ \zeta_{\perp}' &\sim 170 \end{aligned} \right\}. \quad (7.11)$$

The problem of natural splitting is thus rather delicate one and we will not pursue this problem further, since the inconsistency caused by the formula (7.3) is now removed.

## § 8. Conclusion

Although several problems remain unsolved, the main purpose of the present paper, i.e.

crease of the angular momentum in crystals;

$$k' = -\frac{1}{\sqrt{2}} (f_2 x_{\pm} | l_z | e u_{\pm}), \quad (7.6)$$

which is unity for  $e$  and  $f_2$  function constructed from pure  $d$  functions. (7.5) then gives

$$\left. \begin{aligned} k' \zeta_{//}' &= 130 \sim 120 \\ k' \zeta_{\perp}' &= 110 \sim 100 \end{aligned} \right\} \quad (7.7)$$

The formula (7.3) for the expression of  $\delta$  should be reexamined. The shift of the Kramers doublet due to the perturbation  $\mathcal{H}'$  is given by

the assignments of the absorption bands and lines of ruby Cr<sup>3+</sup>:Al<sub>2</sub>O<sub>3</sub>, has now been achieved. The results and unsolved problems are summarized below.

(a) For the  $U$  and  $Y$  bands the assignments (4.11) has been made. The anisotropy shown by these bands is understood qualitatively, but not quantitatively. The parameter  $K$  which is a measure of the strength of the trigonal field was determined from the splittings of the bands:

$$K = -350 \text{ cm}^{-1}.$$

(b) For  $R_1$  and  $R_2$ , the assignments (5.21) has been made. The anisotropies of the lines are closely related to that of the bands, and this problem needs further investigations. The second order perturbation formula (5.6) leads to the following value of the spin-orbit coupling parameter for  $f_2$  electrons:

$$\zeta = 140 \text{ cm}^{-1}.$$

For  $B_1$  and  $B_2$ , the assignments (5.24) has been made. The separation between  $B_1$  and  $B_2$  could not be correctly given by the formulae (5.16) and (5.18) derived under the assumption

of the strong field limit.

(c) For the assignments of these lines, the analyses of the Zeeman effect offer most conclusive evidences.

(d) The large  $g$ -shifts of  $R_1$  and  $R_2$  excited states observed in the Zeeman patterns have been explained by taking into account the second order correction of the type  $V_{\text{trig}}^2 \cdot L_z$ . The correction is fairly large if the excited state  ${}^2F_1$  lies near  ${}^2E$ . From the sign and the magnitude of the observed  $g$ -shift,  ${}^2F_1$  is expected to lie at the shorter wave-length side of  ${}^2E$  separated approximately by  $\sim 700 \text{ cm}^{-1}$ .

(e) The observed  $g$ -values of  $B_1$  and  $B_2$  excited states have also been explained by introducing the reduced expectation value of the orbital angular momentum (for  $f_2$  orbital) in the crystal. As the value of the parameter  $k$  which indicates such a reduction (6.23), we have

$$k \sim 0.6.$$

(f) The line that corresponds to  $\bar{E}_b({}^2F_2)$  is yet unidentified. The lines corresponding to the split components of  ${}^2F_1$  are also not identified yet.

(g) It has been shown that experimental data on the excited states (optical absorption) can be reasonably connected to those on the ground state (paramagnetic resonance).

(h) As to the problem of intensity, the present theory is not satisfactory in that it is semi-empirical, and it is hoped to establish a theory that could predict the absolute intensities of bands and lines as well as the widths of the bands and the lines which have not been touched upon in this paper.

### Acknowledgements

We should like to express our sincere thanks to Professor M. Kotani for his deep interest in this work and encouragement, and to Professor G. Kuwabara and Mr. A. Misu for their permission to use the experimental data of the absorption bands prior to publication. The authors also wish to express their thanks to the members of Prof. Kotani's laboratory for stimulating discussions.

### Appendix

- AI**)  $(f_2^{3/2} E u_{\pm} | V_{\text{trig}} | f_2^{3/2} F_2 x_{\pm}) = -\sqrt{6} K$   
 $(f_2^{3/2} F_2 x_{\pm} | V_{\text{trig}} | f_2^{3/2} F_1 a_{\pm}) = \mp \sqrt{3} i K$   
 $(f_2^{3/2} F_2 x_0 | V_{\text{trig}} | f_2^{3/2} F_1 a_0) = 0$

$$\begin{aligned} \text{AII)} \quad & (f_2^{3/2} \Gamma M_s M | V_{s0} | f_2^{3/2} \Gamma' M'_s M') \\ & = (-)^{M_s - M'_s} (f_2^{3/2} \Gamma \| V_{s0} \| f_2^{3/2} \Gamma') / \sqrt{2(\Gamma)} \\ & \quad (1/2 M_s | 1/2 M'_s | 1 M_s - M'_s) \\ & \quad \times (\Gamma M | \Gamma' M' F_1 M'_s - M_s), \end{aligned}$$

where  $(\Gamma)$  is the dimension of the irreducible representation  $\Gamma$ .  $(\Gamma M | \Gamma' M' F_1 M'_s - M_s)$  is given in Table VIII of (IV).  $(1/2 M_s | 1/2 M'_s | 1 M_s - M'_s)$  is the Wigner coefficient given in TAS.

$$(-)^{M_s - M'_s} / \sqrt{2} (1/2 M_s | 1/2 M'_s | 1 1)$$

$M_s$	$M'_s$	1/2	-1/2
1/2			$1/\sqrt{3}$
-1/2			

$$(-)^{M_s - M'_s} / \sqrt{2} (1/2 M_s | 1/2 M'_s | 1 0)$$

$M_s$	$M'_s$	1/2	-1/2
1/2		$1/\sqrt{6}$	
-1/2			$-1/\sqrt{6}$

$$(-)^{M_s - M'_s} / \sqrt{2} (1/2 M_s | 1/2 M'_s | 1 -1)$$

$M_s$	$M'_s$	1/2	-1/2
1/2			
-1/2		$-1/\sqrt{3}$	

$(f_2^{3/2} \Gamma \| V_{s0} \| f_2^{3/2} \Gamma')$  are evaluated in IV.

$$(f_2^{3/2} E \| V_{s0} \| f_2^{3/2} F_2) = -\sqrt{6} i \zeta$$

$$(f_2^{3/2} F_2 \| V_{s0} \| f_2^{3/2} F_2) = -3i \zeta$$

$$\text{AIII)} \quad (f_2^{3/2} \Gamma M_s M | V_{s0} | f_2^{3/2} e^4 \Gamma' M'_s M')$$

$$\begin{aligned} & = (-)^{M_s - M'_s} (f_2^{3/2} \Gamma \| V_{s0} \| f_2^{3/2} e^4 \Gamma') / \sqrt{2(\Gamma)} \\ & \quad (1/2 M_s | 3/2 M'_s | 1 M_s - M'_s) \\ & \quad \times (\Gamma M | \Gamma' M' F_1 M'_s - M_s) \end{aligned}$$

$$(-)^{M_s - M'_s} / \sqrt{2} (1/2 M_s | 3/2 M'_s | 1 1)$$

$M_s$	$M'_s$	3/2	1/2	-1/2	-3/2
1/2				$-1/2\sqrt{3}$	
-1/2					-1/2

$$(-)^{M_s - M'_s} / \sqrt{2} (1/2 M_s | 3/2 M'_s | 1 0)$$

$M_s$	$M'_s$	3/2	1/2	-1/2	-3/2
1/2			$-1/\sqrt{6}$		
-1/2				$-1/\sqrt{6}$	

$$(-)^{M_s - M'_s} / \sqrt{2} (1/2 M_s | 3/2 M'_s | 1 -1)$$

$M_s$	$M'_s$	3/2	1/2	-1/2	-3/2
1/2			$-1/2$		
-1/2				$-1/2\sqrt{3}$	

$(f_2^3 {}^2\Gamma \| V_{s0} \| f_2^2 e {}^4\Gamma')$  are given below.

$$(f_2^3 {}^2E \| V_{s0} \| f_2^2 e {}^4F_2) = -4i\zeta'$$

$$(f_2^3 {}^2F_2 \| V_{s0} \| f_2^2 e {}^4F_2) = -\sqrt{6}i\zeta'$$

$$(f_2^3 {}^2F_1 \| V_{s0} \| f_2^2 e {}^4F_2) = +\sqrt{6}i\zeta'$$

$$(f_2^3 {}^2F_2 \| V_{s0} \| f_2^2 e {}^4F_1) = -3\sqrt{2}i\zeta'$$

$$(f_2^3 {}^2F_1 \| V_{s0} \| f_2^2 e {}^4F_1) = 3\sqrt{2}i\zeta'$$

### References

- 1) W. Moffitt and C. J. Ballhausen: Ann. Rev. Phys. Chem. **7** (1956) 107.
- 2) O. Deutschbein: Ann. d. Phys. [5] **14** (1932) 712, 729; Ann. d. Phys. [5] **20** (1934) 828.
- 3) H. Lehmann: Ann. d. Phys. [5] **19** (1934) 99.
- 4) B. V. Thosar: Phys. Rev. **60** (1941) 616; J. Chem. Phys. **10** (1942) 246.
- 5) A. A. Manenkov and A. M. Prokhorov: J.E.T.P. **28** (1955) 762.
- 6) R. W. G. Wyckoff: *Crystal structures*, Interscience Publishers New York, 1948.
- 7) Y. Tanabe and S. Sugano: J. Phys. Soc. Japan **9** (1954) 753, 766. (cited as I and II respectively).
- 8) G. Kuwabara, A. Misu and S. Sugano: to be published.
- 9) W. Moffitt: J. Chem. Phys. **25** (1956) 1889.
- 10) Y. Tanabe and H. Kamimura: J. Phys. Soc. Japan **13** (1958) 394. (cited as IV).
- 11) J. Owen: Proc. Roy. Soc. **A227** (1955) 183.
- 12) J. H. Van Vleck: J. Chem. Phys. **7** (1939) 61.